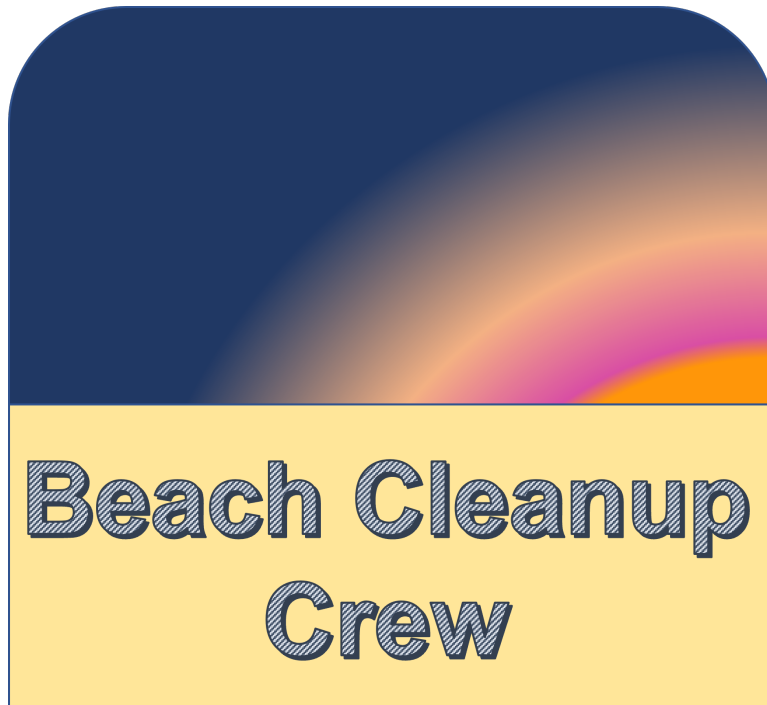


Beach Cleanup Crew

Beach Scrubber



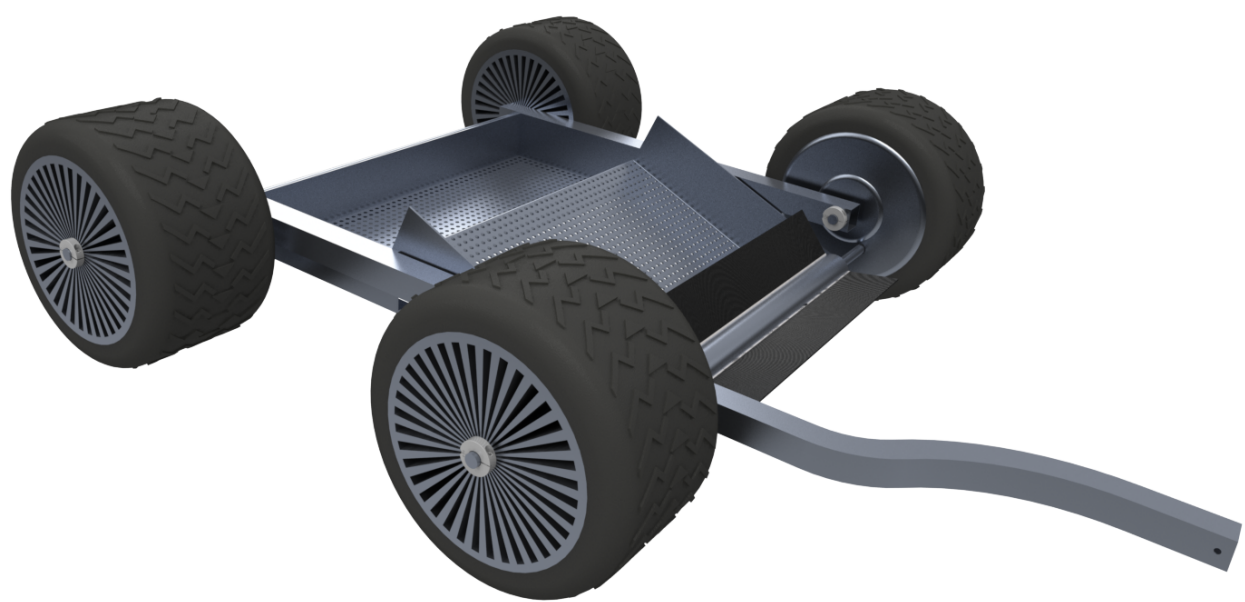
EMA 469: Senior Design
Engineering Mechanics and Astronautics
Department of Engineering Physics
University of Wisconsin – Madison

Authors

Jack Henderson
Nikolaj Hindsbo
Jack Karpelenia
Anshul Yadav

Supervisors

Sonny Nimityongskul
Travis Sheperd
Nivedan Vishwanath



Executive Summary

When tasked with creating a new invention that can help others, The Beach Cleanup crew decided to create a new personal device that can be attached to a bike for cleaning beaches. Beaches can often become incredibly polluted, and so the team's invention will help those who want to help the environment in a more cost-effective manner than current solutions.

In the brainstorming phase, several designs were compared with a set of goal criteria the group decided upon. The best design was the so-called "Brush" design which would implement the use of a parasitic power system and wheels to traverse sand and collect trash. The group also chose to implement a sifting mechanism from the "Sled and Sifter" design to improve the overall performance and to keep sand from being collected.

During analysis, several important calculations were done to make sure the design would perform optimally as well as adjusting some design elements to calculations. Some important analyses covered were the coefficient of rolling friction, the gear ratio for the power system, different load scenarios, vibrational modes and thermal analysis. In conducting these calculations the prototype could then be created.

In the prototyping stage, the brush design was created. Several manufacturing techniques were implemented to create a simplified proof-of-concept prototype. One key challenge in prototyping was the re-purposing of a manual push mower a.k.a "Reeler". Many of the components were reused and some had to be changed to fit the form of the prototype. One part of manufacturing that could have been done differently with a larger time frame is manufacturing more parts to the specification. However, the group was able to get a working prototype to a 1:2 scale and learn a lot from it.

As the prototype was being created, the overall product design was also being refined. Several key components in the newer design are a tire with treads and a fleshed-out sifting plate with a ramp that can be made using one piece of sheet metal. In the prototype, several pieces of metal were fused together making the manufacturing process take a little longer. The design can still yet be improved and has gone through multiple stages of re-design sparked by the new ideas that came from prototyping.

In the future, the group hopes to create a second prototype and test its functionality based on the new design. The prototype could then be further improved by comparing the data collected with targets the group decided in performance. Further refinement of the design is all part of the process and with that, the environment becomes a little bit cleaner-one beach at a time.

Contents

1	Introduction and Problem Statement	5
2	Product Design Specifications	6
2.1	Performance	6
2.2	Size & Weight	6
2.3	Environment	7
2.4	Ergonomics	7
2.5	Cost	7
3	Patents and Similar Products	8
3.1	Large Beach Cleaning Devices	8
3.2	Mid-Size Beach Cleaning Devices	9
3.3	Small Beach Cleaning Devices	9
4	Standards for Design	11
5	Preliminary Designs	12
5.1	Sled and Sifter	12
5.2	Conveyor Belt	12
5.3	Brush	13
5.4	Bucket Collection	15
6	Design Selection and Final Design Concept	16
6.1	Design Criteria	16
6.2	Design Matrix	16
7	Final Design Concept	18
8	Analysis	19
8.1	Analysis 1 - Coefficient Of Rolling Friction	19
8.2	Analysis 2 - Gear Ratio and Brush Rotation	24
8.3	Analysis 3 - Relating Shaft Height to Hitch Attachment from the backend .	27
8.4	Analysis 4 - Load Cases For Hitch Tube	30
8.4.1	Analysis 4.1 - Acceleration From Rest Load Case	30
8.4.2	Analysis 4.2 - Vertical Shock Loading	33
8.5	Analysis 5 - First Vibration Mode of a Flat Plate	38
8.5.1	Calculations for the Perforated Plate	39
8.5.2	Modal Finite Element Analysis	40
8.6	Analysis 6 - Thermal Analysis for Gear Compatibility	41
8.6.1	Radial Compatibility	41

8.6.2	Angular Compatibility	42
8.7	Analysis 7 - Shear Analysis of Axle	43
9	Final Design	46
10	Manufacturing Considerations	48
10.1	Main Frame	48
10.2	Sifter and Ramp	49
10.3	Wheels	51
10.3.1	Back Wheels	51
10.3.2	Front Wheel	51
10.4	Bristles	52
10.4.1	Attachment to Roller	53
10.5	Front Axle and Roller	55
10.6	Back Axle	56
11	Prototype	57
12	Conclusion	61
12.1	Lessons from Design	61
12.2	Lessons from Prototype	61
12.3	Evaluation of Design Criterion	62
12.4	Future Design Iterations	62
References		66

1 Introduction and Problem Statement

In 2020, nearly 2.6 million pounds of trash was collected along the U.S. coastline [1]. Moreover, this is not a problem that is limited to the U.S., and the growing pollution is becoming especially bad when plastics wash up from the ocean onto beaches. An example of this is in two of Mumbai's dirtiest beach fronts where a beach cleaning organization removed over 190 million pounds of trash from only two beaches in a seven-year span [2]! As Engineers, there is a responsibility to design solutions for sustainability. Today's beaches need a helping hand.

The Beach Cleanup Crew's (BCC) product aims to clean and maintain the beaches to protect the environment. While there are currently a few solutions to cleaning beaches, these are either handheld and take time or large machines that can cost tens of thousands of dollars. This problem is especially detrimental to countries where the economic benefit from clean beaches is too small to pursue. Research done by the South African Journal of Science has come to the conclusion that their beaches will continue to accumulate litter unless cheaper methods of cleaning beaches are invented Africa [3]. The BCC will make a device that would bridge this gap. The proposal is for a system that can filter unwanted debris such as small-to-medium-sized general ocean debris, litter, and feces that can get in the way of enjoyment at the beach. This would save money for clients, such as private beach owners, activists, and government municipalities. when compared to heavy machinery, the cost is reduced. And when compared with small, hand-held machinery, the BCC's project will save time with faster beach cleaning.

2 Product Design Specifications

Product Design Specification (PDS) is an essential part of the design process which highlights what the product is required or intended to do and the scope of the product. The PDS will provide direction throughout development. The following subsections will describe the most important design specifications that the group identified. Specifically, the criteria listed below were specified for the cleaning device to be used attached to a bike because it is the most common and accessible vehicle in the world. If it becomes apparent that all the devices would be too heavy for a biker to comfortably use, the reach then is for the attachment to be able to go on a bicycle. Overall, the beach cleaning device should be faster to use than hand-held devices and the aim is that it can pick up small to medium-sized garbage.

2.1 Performance

Current competition gauges that hand-held devices would be able to clean around half an acre, or about 5 basketball courts to put the measurement in perspective, per hour depending on if it is motor-led or purely mechanical[4]. With that in mind, the team is aiming for the device to be able to clean just under one acre per hour and have enough disposal collection capacity for 15 minutes of use at a representative beach. The goal is that the cleaning device should be able to collect medium objects such as bottles, cans, food wrappers, and if possible also some smaller items such as straws, coins, and so on. As a baseline measurement, small debris is approximately under one cubic in size and medium debris would be approximately one to 30 cubic in. Secondly, the device needs to return sand to the beach but would end up picking up rocks that fall into the size category for target debris. For that reason, this device is not intended to be used on a rocky beach as it is possible that removing rocks from a beach may be unlawful in some areas.

2.2 Size & Weight

According to bikers' experiences, "someone in a reasonable physical condition" can comfortably pull a 600 lb load on level ground at 8 mph or 1000 lb at 6 mph [5]. Their math of rolling resistance is related to the coefficient of rolling resistance which is listed as 0.006-0.010. However, sand is considerably different, with typical rolling resistance coefficients of 0.04-0.06 for car tires on solid sand and 0.2-0.4 for car tires on loose sand [6]. Therefore, at 7 mph the build should be constrained to approximately 30 pounds in weight when towed behind a bike. As for size, the device is expected to be approximately 24" wide and should be able to fit in a truck bed (four feet by four feet) length-wise for transportation. Furthermore, it should be possible for the user to lift the cleaning device into a truck bed. For lifting,

the group intends to follow OSHA's recommendation of the NIOSH Lifting Equation for an individual: 50 pounds at a maximum height of 55 in.

2.3 Environment

The beach cleaning device could be exposed to salt water, sand, and many other elements. The *Beach Scrubber* is intended for use on the dry part of the sand, but it would be naive to think that it will not be in contact with water. Therefore, the group plans to use 5000-6000 series aluminum because it is lightweight and corrosion resistant [7]. Furthermore, the group is using the Florida Ordinance 00-10 for Fort Myers Beach as a basis for tire pressure. To limit damage to wildlife, tire pressure should be lowered to 10 psi for travel on sand [8]; this should not affect performance anyways because a suggested tire pressure for fat tire bikes starts at 10 psi [9].

2.4 Ergonomics

Ease of client use is an important factor for the design process. The *Beach Scrubber* should be simple enough that anyone with a bicycle would be able to assemble it and start cleaning in a short amount of time. To be specific, the trash collection system should be easily detachable from the cleaning device. It should also be comfortable for the client to attach, reattach, and stow away in a truck bed. The previous factor ties into size and weight as well, it needs to be light enough that a client can carry it with relative ease and small enough that, when disassembled, it can be stored in a four-foot by four-foot area.

2.5 Cost

Lastly, cost is another important factor to take into account when designing and manufacturing the *Beach Scrubber*. The goal is to make the device accessible to anyone who wants to take action cleaning up beaches. Fat tire bikes, which would be the most likely option for use on a beach, have a price range that starts at around \$400, so the product has an innate cost in that the customer can afford or already owns a fat tire bike. As such, the product will have a price point of around \$500 omitting that manufacturing costs are greater.

3 Patents and Similar Products

Beach cleaning products are a niche product, and as such, there are not that many existing variations of beach cleaning devices and/or attachments. The existing beach cleaning products tend to be either very large or very small with only a few mid-sized models, which are engine-powered. There are small, hand-held devices meant to cover a much smaller amount of land area (i.e. a beach volleyball court which is typically 30x60 feet) and there are large, tractor-pulled products meant for commercial use in places such as large, city-owned beaches. There are a few products in the mid-sized range, but they are engine-powered more often than not. The goal here is to design a product in that mid-range of sizing that is not powered by an engine in the product itself.

3.1 Large Beach Cleaning Devices

The most advertised tractor-pulled products seem to be those from H. Barber and Sons (shortened here on out to “Barber”) [10]. Its beach cleaning products have been used more than any other company in the world with its beach rakes being used on six continents and in over 90 different countries. Their cleaners in the Surf Rake line have a 6-7ft width with operating speeds of 1-15 mph and are capable of cleaning 4-8 acres/hr depending on the specific product used [11]. The general design for Barber’s large beach rakes is shown below in Figure 3.1.1.

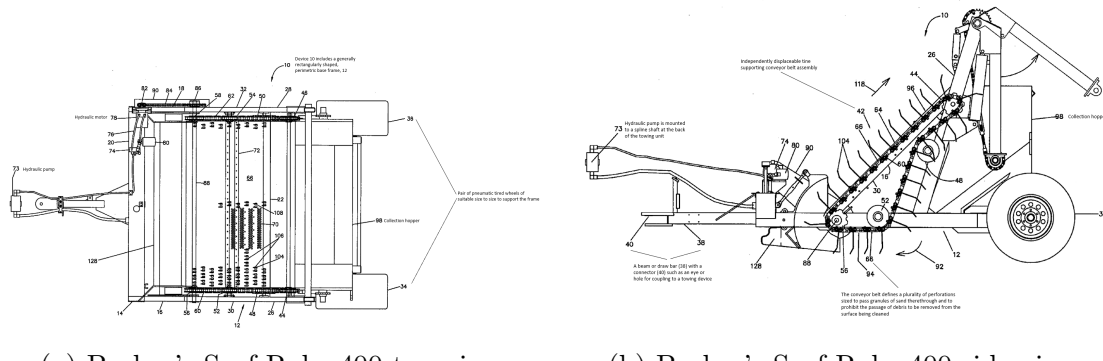


Figure 3.1.1: Barber's Surf Rake 400 design drawings [10].

These products are designed to be pulled by 4-wheel drive agricultural type tractors having real wheels in the range of 28-30in and power take out (PTO) ranging from 30-60 horsepower depending on the specific design. The larger Barber designs are great for companies or organizations where cleaning a large land area is required, but they are not feasible designs for the goals of this project.

3.2 Mid-Size Beach Cleaning Devices

There are a few mid-sized beach cleaning products out there, most of which are engine-powered, walk-behind designs. The popular versions of those walk-behinds are Barber's Sand Man series and the Delfino Walk Behind distributed by CleanSands, Inc. Both are self-propelled beach cleaning products with similar performance specs. The Sand Man 850 has a working width of 33" and a working speed of 1.1-3.4 mph to produce an area cleaned between 0.35 and 0.79 acres/hr while the Delfino has a working width of about 29.5" and is capable of cleaning 0.62 acres/hr [4], [12]. Both products use the same 5.5 Hp 4-stroke Honda engine. These beach cleaning designs are ideally used for volleyball courts, sand bunkers, playgrounds, small-to-medium-sized beach areas, etc. These products are shown below in figures 3.2.1 and 3.2.2. They are certainly a good option if the budget allots, but they are still straying from the goal of having a small-to-midsized option that is towed by a bicycle rather than being self-propelled



Figure 3.2.1: Barber's Sand Man 850 self-propelled sand cleaning device [4].



Figure 3.2.2: CleanSands' Delfino self-propelled sand cleaning device [12].

3.3 Small Beach Cleaning Devices

Of the small, hand-pulled devices on the market, the most appealing device looks to be the Sandragin manual sand cleaning tool provided by CleanSands, Inc. It is designed to

clean, groom and comb any sand area in need of a quick and quiet touch-up. It is designed to be ideally used for tasks such as sifting/grooming between beach volleyball matches, cleaning things like cigarette filters that find their way to the sand around places like tiki bars, etc. It is currently provided in 18" and 24" working widths and is completely made from aluminum for lightweight and durability[13]. As with every beach cleaning product, it has its best results when the sand is well dry. The Sandragin is a great device for smaller land areas, but it again falls short of the targeted goals and is on the opposite side of the spectrum than the capabilities of the larger devices. Figure 3.3.1, shown below, provides visuals for the description of the device.

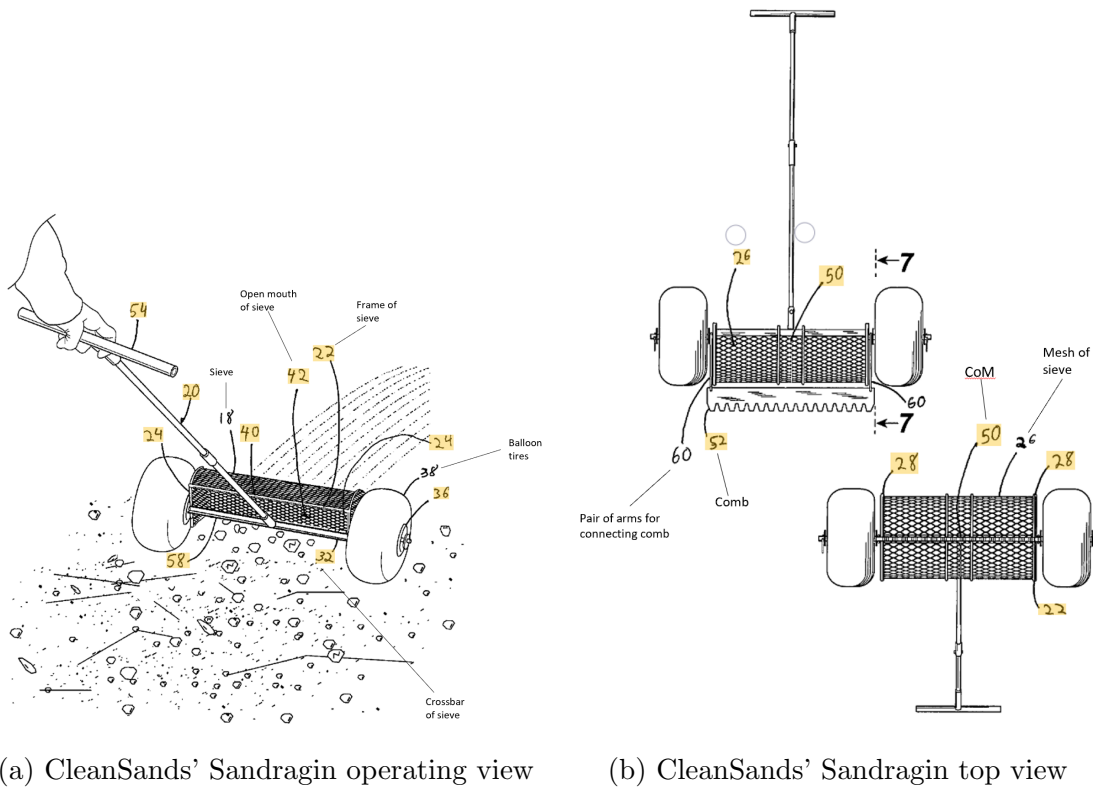


Figure 3.3.1: CleanSands' Sandragin manually pulled cleaning device [14].

The operation of the Sandragin is mostly user-friendly with a couple of areas with room for improvement. First, the mesh is dragged along and has a small carrying capacity that must be emptied frequently. Second, if the user is not dragging along the Sandragin at an acceptable angle, the mesh will not drag below the surface to collect debris. A positive aspect of the device is the included rake which drags behind the mesh and makes the sand look neat and groomed.

4 Standards for Design

With the design of a tool to help clean beaches, there are a number of standards to follow. When dealing with sand and the environment, standards are designed to protect the environment and make manufacturing more universal. The first consideration is the allowable pressure distribution on beaches. For this, the group chose to abide by Florida Ordinance 00-10, which states that beach vehicles must have a maximum pressure of 10 psi where tires contact the sand [8].

The vehicle not only needs to operate safely with respect to the environment, but it also needs to be able to withstand the environment it operates in. MIL STD-810 gives a testing framework for the survivability of the vehicle in sandy environments, thus allowing the team to design the vehicle to prevent corrosion, abrasion and other types of damage that reduce the lifespan of the product [15].

For manufacturing of the device certain standards should be followed to ease the manufacturing process. In the design of the product, some parts and assemblies should be attached together by welding. For this process AMS2685 is followed. AMS2685 describes standards for Tungsten Inert Gas (TIG) Welding and the group decided that 4043 aluminum rods as the filler metal because of the price and that aluminum is the primary metal being welded [16].

Finally, for the parts and assemblies that are not welded together all other fasteners will follow ASME B1.1, which defines threads, tolerances, and nomenclature for unified screw threads [17]. This standard is important in keeping consistency within manufacturing so that the number of different types of screws can be kept to a minimum.

5 Preliminary Designs

There are four different preliminary designs for beach cleaning attachments. The primary difference between these four concepts is the way they interact with the sand and sift through the garbage. The preliminary designs interact with sand through a combination of brushing and plowing using side skis, conveyor belts, and a bucket for garbage collection.

5.1 Sled and Sifter

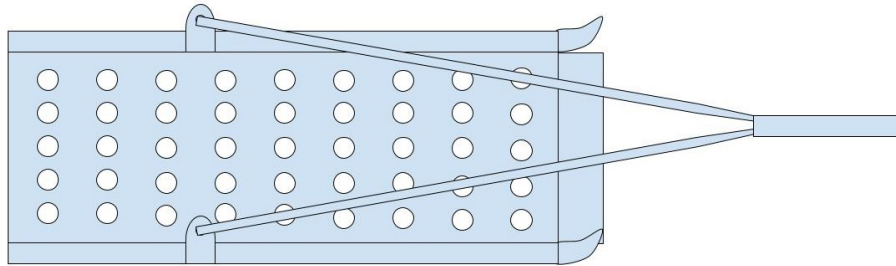


Figure 5.1.1: Concept drawing of a sifting device attached to sleds.

The first design, shown in Figure 5.1.1 consists of a perforated sifting plate with a protrusion that plows the beaches, collects the sand/garbage mixture, and sifts it through the sifter for filtration. The sand gets filtered back onto the beach and the garbage is collected in a trash bag behind. The idea of this design comes from plow that plow farms. The inertia of the mass build-up on the underground plate pushes material on the sifting plate. A decline on the sifting plate allows for gravitational motion toward the back with sand being sifted out.

5.2 Conveyor Belt

The second design, shown in Figure 5.2.1 on the next page, is similar to the first as both have a plate that plows the ground. This design, however, then passes the sand/garbage mixture to a rotating conveyor belt which is perforated. The conveyor belt could be electrically controlled through an adaptor to the bike or batteries. Alternatively, the conveyor belt could be geared to the rotation of the device's wheel through a gearing mechanism. The sand falls down due to spring-induced vibrations and the garbage is collected in a trash bag behind. This design ensures that the material on the front moves back which may not be the case in design one.

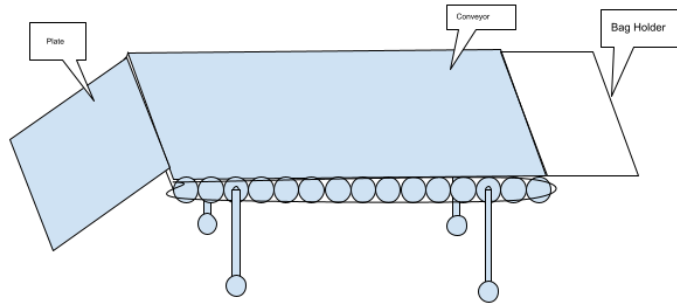


Figure 5.2.1: Concept drawing of a conveyor belt sifter.

5.3 Brush

The third design builds upon the first one by attaching a rotating brush in the front. This design excludes the plowing plate and instead relies on the brush to facilitate the motion of the garbage sand mixture onto the sifting plate.

The thought process behind the brush is inspired by those devices seen on campus that clean sidewalks. By rotating clockwise towards the sifter, it should be able to cause motion in the sand and hit larger objects such as bottles, rocks, and sticks and encourage the collection of material on the sift. Additionally, this will hopefully reduce the drag force of the cleaning device as the device no longer plows through the beach. The drawing of a brush-based concept is shown in Figure 5.3.1.

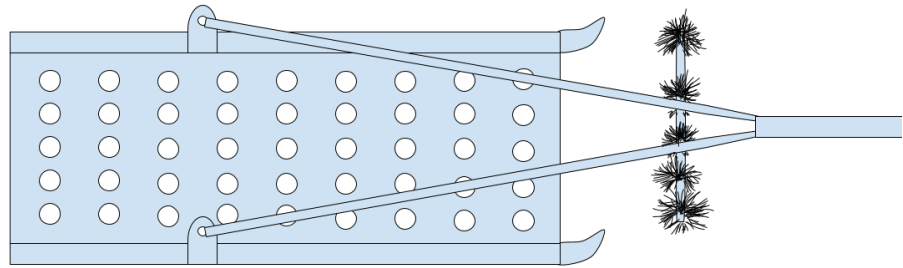


Figure 5.3.1: Concept drawing of brush sweeper.

5.4 Bucket Collection

The final design is different from the previous three since it does not have a sifting plate. Instead, it has a perforated blade that is dragged along. The blade plows the sand and the holes in it allow for beach sand to pass. Material that is collected but not sifted is then transported to the bucket periodically. The bucket could be electrically controlled through motors or mechanically controlled with a person lifting up the blade every so often. The concept drawing is also shown below in Figure 5.4.1.

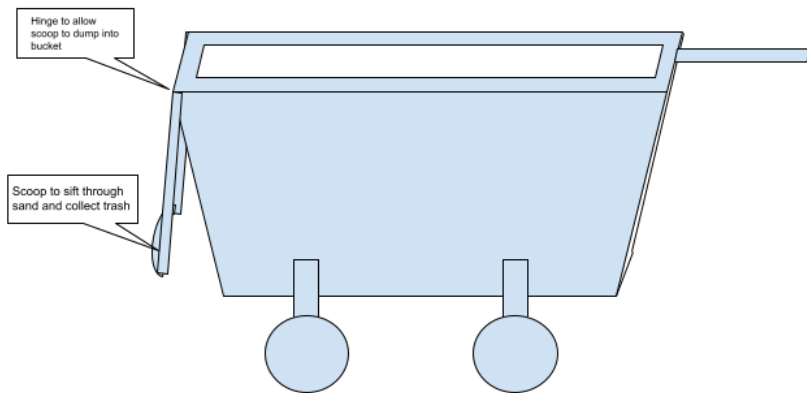


Figure 5.4.1: Concept drawing of a bucket sift with a receptacle.

6 Design Selection and Final Design Concept

In order to narrow down design ideas in an objective manner quantitatively, five criteria were identified as important and were weighted on a scale from 1-5 based on importance. The importance of criterion was highlighted by its influence.

Each design was also given a 1-5 rating in each category. Multiplying the rating of each category by the influence of that category and summing them up gave the overall rating. The criteria are given in section 6.1 and the design matrix with ratings and influence is given in section 6.2.

6.1 Design Criteria

The five main design criteria that were considered were **Weight**, **Complexity**, **Ergonomics**, **Efficiency**, and **Cost**.

Weight is the most important criterion. This is the metric that quantifies the difficulty in moving the device. Of course, that includes the actual weight of the system but it also includes friction and drag since these forces make the device more difficult to move. A good rating in this category means that the device is easy to pull and the overall **weight** of the system is minimized. Furthermore, this criterion adheres to Florida Ordinance 00-10.

After weight, complexity and efficiency are the two most important criteria. Complexity is a measure of the difficulty of designing and subsequently manufacturing the device. A design that is easier to design and manufacture and overall less complex, gets a more favorable rating on complexity.

Efficiency is a measure of the device's ability to pick up varying kinds of trash in the fastest manner possible. Of course, the team wants to design the device for performance which affects marketability and appeal. The designs are rated based on how the team predicted they would perform in a test setting. Efficiency is probably the most subjective category, but is still nonetheless, necessary.

Ergonomics was determined as the least important factor in the design matrix. Ergonomics is a measure of the ease of use of the customer. It specifically excludes the interactions defined by weight and efficiency categories but instead includes things like the user's action for trash disposal, any setup that would be required from the user etc.

Lastly, the cost is a factor that makes its way into any design conversation and this is no exception. The overall cost of the product is important because consumers will not buy a product designed to clean the environment if it is too expensive.

6.2 Design Matrix

The previous five categories all culminate into the design matrix. The team determined, through rigorous discussion, how each category is weighted and what each design

scored in every category. The results are shown in Table 6.2.1.

Table 6.2.1: Design matrix for evaluating the preliminary concepts

Category	Influence	1-Sifter	2-Conveyor	3-Brush	4-Bucket
Weight	5	1	2	5	3
Complexity	3	5	2	3	3
Efficiency	3	4	4	3	2
Ergonomics	1	5	4	2	3
Cost	2	5	2	4	3
Total		47	36	53	39

Cells in the Table 6.2.1 highlighted in green indicate the top score in each category. It would seem that the sifter was the best design, however, the brush with sifter weighted above the sifter mainly due to its advantages in the weight category as plowing the beach would have created significant frictional and drag forces. While the sifting idea excelled in complexity, efficiency, and cost, the brush idea is very similar except with a degree of extra complexity and costs in the brush mechanics. Going with this idea it is expected to create less drag at a slight cost in efficiency and maintenance for the user who would also be expected to clean the brush. The group believes that the sifter would create too much drag for a user to comfortably use on a bicycle, which was an important consideration. If the brush design seems to be not feasible for bike transportation, the weight consideration would be less important and the sifter could be very very favorable.

While the bucket and sifter were close runner-ups, the conveyor belt seems to lack behind in most of the ideas because it would be a complex, heavy design. The bucket also fell behind because it did not excel in many formats and is complex. Additionally, in the time that the bucket would go up and down, it would lose some efficiency.

7 Final Design Concept

The team decided to use a combination of the four designs presented to come up with the overall design. The final design includes wheels instead of skis like the conveyor belt design to minimize the weight. The final design also includes a brush but excludes the plowing plate. This means that the design is only capable of collecting surface-level trash. The team presumes that partially submerged trash would be imparted with enough energy to be lifted out of the ground and collected. Finally, the design would be incapable of collecting trash that would be completely submerged. Figure 7.0.1 shows a rough sketch of the design that the team has come up with.

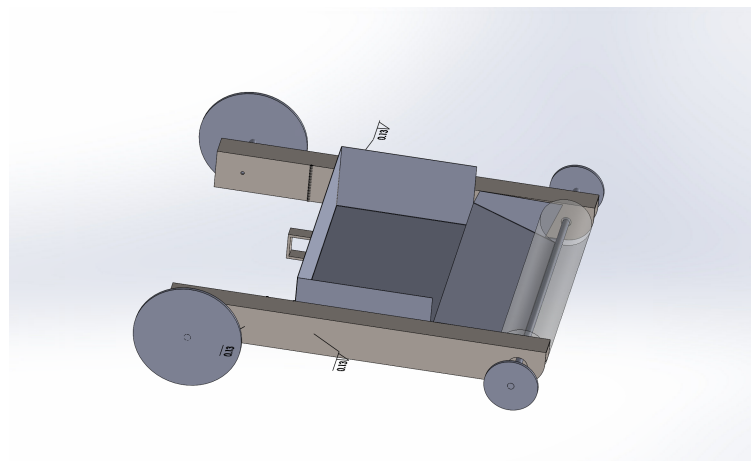


Figure 7.0.1: The SolidWorks design the team is planning to prototype

As the astute reader may observe the CAD is incomplete and has a lot of grey areas. For example, the CAD offers no information about the rotation of the brush which could be achieved by an electrically powered motor that would be independent of the tire rotation or could be powered through an inner gear pinion mechanism. Furthermore, it is unclear if the wheels are going to be of the same size or not, but it is better to presume that the size would probably not be the same. Lastly, the sifting plate does not contain any holes because currently, the size of the holes or the spacing between them is unknown.

Therefore, 7.0.1 is a purely conceptual CAD that the team used as a baseline. This was refined many times to come up with the final design.

8 Analysis

An important part of the design process before building and testing any prototype is making sure the concept can work on paper. Some key ideas in the analyses that the group performed are ensuring the device can roll on sand easily, that the hitch attachment will not tip over the device, and determining the proper gear ratio. The purpose of some of the analyses was to put restrictions on various dimensions while others were performed to ensure stability, compatibility and assurance that the design would work as described without fail.

8.1 Analysis 1 - Coefficient Of Rolling Friction

An important part of the group analysis was confirming a coefficient of rolling resistance of friction through both experimental and accepted values. This is vital to analysis for a variety of reasons. Firstly, the design is centred around a bike with the limiting factor being how much a person could tow in sand comfortably. Biking in the sand is already hard, so the frictional resistance in sand from the cleaning device will be the most important consideration of the weight limit of the device. Secondly, rolling resistance is dependent on the types of tires, the radius of the wheel, sand conditions, and many other factors. As an example, the coefficient of rolling friction can be defined as dimensionless similar to traditional friction coefficients; however, it can also be dimensional in relation to the wheel radius (r). In the analysis, the group will focus on the dimensionless quantity because the wheel radius of the experiment and final design are close. Equation(8.1) quantifies the dimensionless relation, where μ is the coefficient of friction, N represents the normal force, and F_f represents the force of friction [6].

$$F_f = \mu N \quad (8.1)$$

Because of variations of rolling resistance coefficients and no specific values or rolling resistance for the desired scenario, it was necessary to design an experiment to find a reasonable coefficient of rolling resistance for the cleaning device wheels that the group will use. Table 8.1.1 contains experimentally found values of rolling resistance, c , and a dimensionally dependent value, c_l . The table provides a good estimate to compare the experimental values with.

Table 8.1.1: Rolling Resistant Coefficient Values From Engineering Toolbox [6].

Rolling Resistance Coefficient		
c	c_f (mm)	
0.001 - 0.002	0.5	railroad steel wheels on steel rails
0.001		bicycle tire on wooden track
0.002 - 0.005		low resistance tubeless tires
0.002		bicycle tire on concrete
0.004		bicycle tire on asphalt road
0.005		dirty tram rails
0.006 - 0.01		truck tire on asphalt
0.008		bicycle tire on rough paved road
0.01 - 0.015		ordinary car tires on concrete, new asphalt, cobbles small new
0.02		car tires on tar or asphalt
0.02		car tires on gravel - rolled new
0.03		car tires on cobbles - large worn
0.04 - 0.08		car tire on solid sand, gravel loose worn, soil medium hard
0.2 - 0.4		car tire on loose sand

Notable values from the table include a dimensionless coefficient rolling friction value between 0.2-0.4 on loose sand and 0.04-0.08 on solid sand. As a reference, bike tire on asphalt is measured as 0.006-0.01, so there is a significant difference between sand and road conditions. As talked about before, the group decided to do an experiment to ensure that these values are reasonable in sand conditions.



Figure 8.1.1: Experimental Setup for Determination of Rolling Resistance and Angle Measurement

In order to collect values, the group went to the sand courts at Dejope where conditions of the sand can best be explained as extremely loose sand. Then, a force gauge was attached to the reeler shown in Figure 8.1.1 (pulling by hand) and different weights were attached to the reeler to expand this test for multiple weights of the system. The reeler was dragged at as constant a speed and angle as possible. A stopwatch was used to justify the constant speed approximation for experimentation. A baseline average time for each speed was taken and if the times were too far off then the test was scratched.

There were some limitations to the experiment that should be addressed. Firstly, the only way to drag the reeler with the larger front wheels on the ground also engaged blades to move from the pinion interaction, so it should be noted that there was additional friction from the blades along with the rolling friction. Therefore, the coefficient of rolling friction measured is going to be larger than the actual. Secondly, the wheels used from the reeler are not ideal for sand - they are thin and meant to be on hard surfaces such as the ground, so the ridging pattern was small. Both of these factors will cause the coefficient of rolling friction values to be overestimated. The force varied significantly over the distance because of the nature of the sand. When hitting bumps the force went up to 10-40% of its nominal value depending on speed. Higher speeds saw larger force increases as the plate would briefly take off the floor.

Therefore, the group used the average of ten random points in the video of the force gauge along the constant distance to record the average force that the gauge was displaying for each speed. From this average force, the analysis shown on the next page relates the force on the gauge to the dimensionless coefficient of friction at each weight.

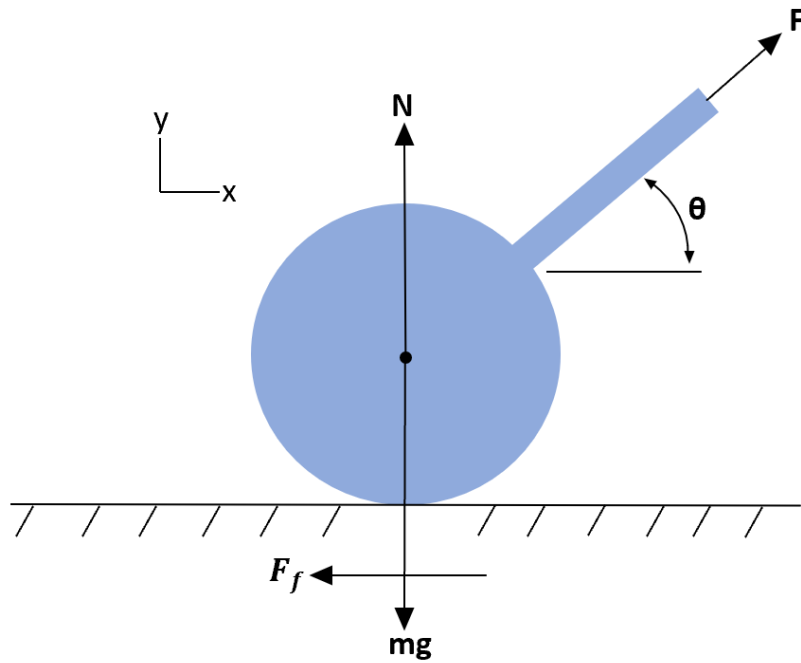


Figure 8.1.2: FBD of the Experimental Setup [18]

Figure 8.1.2 defines F as the applied force by the user, θ as the angle of the reeler, N as the reeler's normal force, mg as the weight of the reeler, and F_f as the force of friction the reeler would experience. Using static conditions (constant speed), the coefficient of rolling friction can be interpreted from the data collected by solving equilibrium equations in Equation 8.2. All experiments were performed at a $\theta \approx 45^\circ$

$$\begin{aligned}
 \sum \vec{F} &= 0 \\
 \sum \vec{F}_x \cdot \hat{x} &= F \cos(\theta) - F_f = 0 \\
 \sum \vec{F}_y \cdot \hat{y} &= F \sin(\theta) + N - mg = 0
 \end{aligned} \tag{8.2}$$

The normal and friction forces can be determined by re-arranging 8.2 in Equation 8.3

$$\begin{aligned}
 N &= mg - F \sin(\theta) \\
 F_f &= F \cos(\theta)
 \end{aligned} \tag{8.3}$$

Using Equation 8.3 and, the friction force can be determined using the definition of friction in Equation 8.1.

$$F_f = (mg - F \sin(\theta)) \cdot \mu_R \tag{8.4}$$

From Equations 8.3 and 8.4, μ_R can be solved.

$$\mu_R = \frac{F \cos(\theta)}{mg - F \sin(\theta)} \quad (8.5)$$

Where m and F are data points collected in the experiment. The group inserted the data collected into Matlab code shown in 8.1.3 to solve for the average dimensionless coefficient of friction.

```

1- F = [8,9,10,12.5,14]; % Average force [lbs] at constant speed
2- mg = [19.27, 21.87, 24.54, 27, 29.5]; % Measurements of weight [lbs]
3- angle = pi/4; % Angle approx 45 degrees
4- radius = 1.791667./2; % Radius of the wheel in feet
5- mu_r = F.*cos(angle)./(mg-F.*sin(angle)); % Dimensionless coefficient of friction
6- total_mu = sum(mu_r)./5; % Average Dimensionless coefficient of friction
7- disp("Average Dimensionless Friction Coefficient");
8- disp(total_mu)

```

Average Dimensionless Friction Coefficient

0.4445

Figure 8.1.3: Experimental Setup and Angle Measurement

The average forces and weights collected from the experiment can be seen in the first two lines of Figure 8.1.3. Measurements of force and weights are in pounds. Using the Equation 8.5 the dimensionless coefficients of rolling friction were calculated for each test. The average dimensionless friction coefficient found was approximately 0.44. Therefore, it would be reasonable to conclude that the rolling resistance values online from 8.1.1 are in a reasonable range. As explained in the limitations, the tire width, type, and radius all impact coefficient of rolling resistance as well, and the factors of the experiment should have overestimated the friction coefficient. The values collected were for a car tire in loose sand. Car tires are not ideal in sand and loose sand is the type of sand that has the highest coefficient of friction. Therefore, a dimensionless coefficient of rolling resistance of 0.3 for loose sand would be a great guess and will be used by the group when designing weight limitations. Potential consequences of under-estimating the coefficient of friction would be that the product would drag more than expected and at the worst case render the product useless if the client cannot drag it. Not all sand is loose sand but nonetheless designing around worst-case will make sure that the cleaning device can be used.

According to biker's blog, the average rider can comfortably tow 1000 lbs with a rolling resistance of 0.01 at 6 mph with a typical mountain bike [5]. With 0.3 as the benchmark for loose sand it can be expected to comfortably tow the cleaning device from frictional forces alone if the device weighed up to 33 lbs.

8.2 Analysis 2 - Gear Ratio and Brush Rotation

Another very important analysis that had to be done was asking the question: how fast does the brush have to spin for the cleaning device to work? And how much of a minimum gear ratio should the device have to make this possible?

In order to answer this question, the group did an analysis on the brush to identify the minimum gear ratio that the brush should have in order to launch debris up a 1-foot height ramp into the garbage collection system, which is the current assumed height of the collection device.

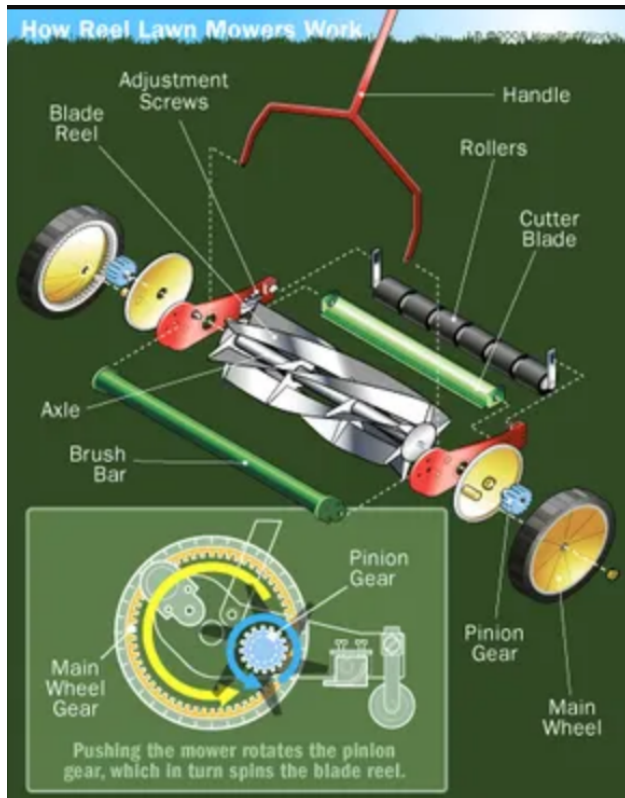


Figure 8.2.1: Reel Mower Expanded View [19]

The cleaning device will be using a pinion interaction similar to a reel mower so that the brush axle can spin at a faster angular velocity than the outside wheel. Since the brush is cleaning up debris from the floor, the cleaning device brush length will be designed so that it barely touches the floor when vertically down. That is, $R_{Wheel} \approx L_{Brush}$ (minus the axle and roller radius for the real design, but for intents of the analysis this assumption will hold true because $L_{Brush} \gg R_{Axe+Roller}$). Analogous to the reel mower, the cleaning device brush has a similar function as the blades in Figure 8.2.1.

This Analysis makes the following assumptions:

- The debris sticks to the brush and is launched at the relative speed at which the end of the bristle is moving before it touches the stationary debris
- The angular speed of the brush remains unchanged after collision
- The bristles do not touch/interact with the ground
- Friction and drag forces are negligible

By Design choice, the radii of all four wheels are the same (6.5 in) the height of the ramp and subsequent chassis as 6.5in (h). The angle that the ramp makes with the horizontal is not of relevance in the upcoming energy calculations since all forces are conservative and friction and drag are neglected. The user on the bike and the center of the wheel are moving at 6 mph or 8.8 ft/s.

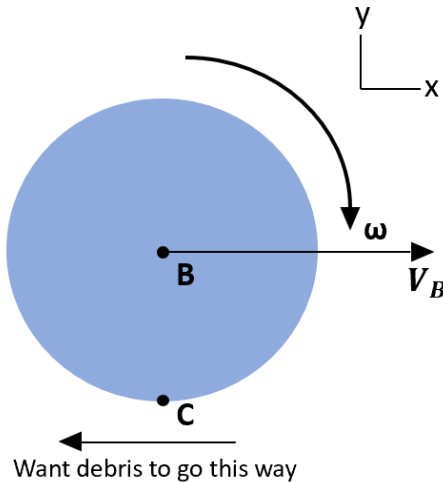


Figure 8.2.2: Relative Motion and Angular Velocity Of the Brush

$$\vec{v}_c = \vec{v}_b + \vec{\omega} \times \vec{r}_{c/b} \quad (8.6)$$

v_B is the velocity of the bike, v_C is the velocity of the bristle right before it touches the debris and also v_C is the velocity of the debris by after the collision, by assumption. R is the radius of the wheel and ω is the angular velocity of the wheel.

An energy balance is performed to determine the minimum velocity at point C v_c that is required to raise the debris over the ramp assuming that the debris was initially at rest and that the energy imparted is just enough for the debris to reach the ramp height h . The LHS of Equation 8.7 is the potential energy the debris would need to overcome. The RHS of 8.7 represents the kinetic energy of the debris right after the debris is hit by the brush.

$$mgh = \frac{mv_c^2}{2} \quad (8.7)$$

Solving the Equation8.7 for v_C gives $v_C \approx 3.26 \text{ ft/s}$.

This velocity is in the -x direction relative to the ground, which will be used in Equation8.6 to find the minimum angular velocity (ω_{brush}) at which the brush must move to achieve this velocity can be calculated using Equation8.6.

$$-3.26 \frac{\text{ft}}{\text{s}} = 8.8 \frac{\text{ft}}{\text{s}} - \omega_{brush} \frac{\text{rad}}{\text{s}} r \text{ft} \quad (8.8)$$

Solving Equation8.8 for a wheel radius of 6.5 in. the minimum angular velocity is 22.26 rad/s for the brush.

Now, the brush is attached to the wheel with a pinion interaction, so in order to ω of 22.26 rad/s, it will need at least a certain gear radius. This value can be calculated by relating the wheel's angular velocity to that of the brush. If the bike is traveling with 6 mph (8.8ft/s) in the +x direction then the angular velocity of the wheel (ω_{wheel}) can be determined using Equation8.6. A reminder that the wheel radius is approximately the same as the length of the brush, which are both 6.5in.

$$8.8 \left[\frac{\text{ft}}{\text{s}} \right] - \omega \left[\frac{\text{rad}}{\text{s}} \right] r \left[\text{ft} \right] = 0 \quad (8.9)$$

Solving Equation8.9 an angular velocity of the wheel of 16.25 rad/s. The gear ratio (GR) can then be determined by relating the two angular velocities.

$$GR = \frac{\omega_{brush}}{\omega_{wheel}} \quad (8.10)$$

Solving out Equation8.10 the gear ratio needs to be at least 1.37. Of course, the analysis made several assumptions such as no friction or air resistance and used ideal solutions such as minimum velocity to get up the ramp. Therefore, the brush will use a gear ratio of at least 2 to account for these assumptions.

The gear ratio can also be defined as the ratio of the number of teeth in the gears. For two gears to be compatible, they need to have the same diametral pitch (DM), which is defined as the ratio of the number of teeth (N) to the pitch diameter (d). In the subsequent discussion, the inner gear is gear 1, and the pinion gear is gear 2.

$$DM_1 = \frac{N_1}{d_1} = \frac{N_2}{d_2} = DM_2$$

$$\frac{N_2}{N_1} = \frac{d_1}{d_2} = GR = 2 \quad (8.11)$$

Therefore, Equation8.11 states that the inner gear's pitch diameter needs to be twice that of the pinion gear. Further restriction on pinion gear is added since it needs to be compatible with an axle of diameter (5/8)in. The inner gear needs to fit inside a rim of about 10in and thus should be smaller than that. The gears included in the drawings satisfy all of these requirements.

The conclusion of the analysis is that the cleaning device brush should use a gear ratio of at least 2. The inner gear should have twice as many teeth as the pinion and should be 2 times the pinion diameter.

8.3 Analysis 3 - Relating Shaft Height to Hitch Attachment from the backend

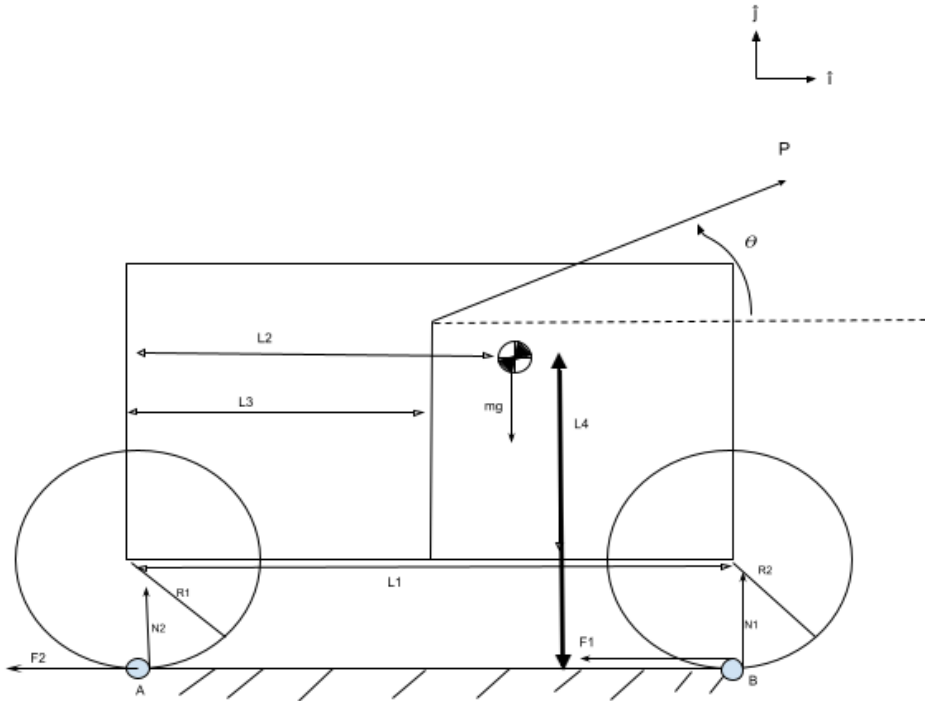


Figure 8.3.1: FBD of the system [18]

The designed structure would experience a lot of external loads such as friction loads, normal forces, weight and the force that the bicycle would apply. These loads may cause the design to tip over such that the front wheels are no longer in contact with the ground. If this happens the gear mechanism would be rendered useless. Therefore, an important analysis was done to determine the relationship between the height of the shaft where the hitch would be placed and the placement of the shaft from the back end, so that the mechanism did not tip. The relations were used to guide the dimensions which were chosen by design.

In order to figure out the position of the hitch attached to the shaft, and the position of the shaft a moment analysis was performed on the system described in figure 8.3.1. Point A is the point at instantaneous rest, (assuming no slip) and the coordinate system is based on this point. l_1 is the x distance between the back and front wheels, l_2 is the x coordinate of the center of mass, l_3 is the x-coordinate of the shaft, l_4 is the y-coordinate of the shaft where the hitch is attached to it at an angle θ . R_1 and R_2 are the wheel radii, mg is the weight of the system, F_1 and F_2 are the frictional forces on the front and back wheels respectively. P is the pull that the user applies and $N1$ and $N2$ are the normal forces that the ground exerts

on the front and back wheels respectively.

The front wheel should not lift from the ground to ensure that the brush is always rotating. The condition that the sum of moments at the back wheel equals zero ensures this. Additionally, this ensures that the frictional forces as well as the normal force N_2 do not play any part in the moment analysis.

$$\begin{aligned} \sum M_A &= 0 \\ N_1 l_1 - mgl_2 - P(\cos(\theta)l_4 - \sin(\theta)l_3) &= 0 \end{aligned} \quad (8.12)$$

Solving for normal force N_1 gives:

$$N_1 = \frac{mgl_2 + P\cos(\theta)l_4 - P\sin(\theta)l_3}{l_1} \quad (8.13)$$

For $N_1 > 0$, implying that the front wheel is in contact with the ground, $mgl_2 + P\cos\theta l_4 - P\sin\theta l_3 > 0$ which can be rearranged to be:

$$\frac{mg}{P} > \frac{\sin\theta l_3 - \cos\theta l_4}{l_2} \quad (8.14)$$

Since the left side of the Equation(8.14) is always positive, the inequality can be easily satisfied if the numerator of the right side is ≤ 0 . In other words, Equation(8.15) ensures that the system remains stable.

$$\tan\theta \leq \frac{l_4}{l_3} \quad (8.15)$$

This analysis implies the following:

- Increasing l_2 increases the stability of the system. Thus the center of mass should be in the front.
- For a large value of l_1 $N_1 \approx 0$ regardless of other forces. Thus the overall length of the system should be minimized.
- For small values of θ , $(0 - 45)^\circ$ the height of the point of attachment can be lower than the distance from the back wheel.
- This approach is very conservative as it does not take into account the relative magnitudes of the Weight and applied forces.

For a more liberal approach, an estimate of force P would be required.

To put an upper limit on P , when $\theta \rightarrow 90^\circ$ and for $N_1 > 0$, Equation(8.14) becomes :

$$P < \frac{mgl_2}{l_3} \quad (8.16)$$

For a system weighing about 33 lbs and $l_2 \approx l_3$, a P value of about 33 lbs is found.

According to pedal power [20], an elite cyclist can exert a power of 5W per unit kilogram of their body weight. Assuming the elite biker weighs 80 kg and bikes at 5m/s on the sand, then the cyclist applies 80 N of force, which is less than 33 lbs, so even an elite biker would not be able to make this system unstable. This force is obviously not completely transferred into pulling the system, but even if it was it would not make the system unstable.

Furthermore, as the angle is decreased, the cyclist can apply a larger force without making the system unstable. The angle is also likely to be smaller than 90° with a hinge attachment on the front wheel. In fact, the angle will be much closer to less than 10° . Nevertheless, even in the worst-case scenario of $\theta \rightarrow 90^\circ$ and $l_2 = l_3 = l_4$, the system does not become unstable even for very large pulling forces.

In lieu of this analysis, the design of the system has the hitch attached to the front dead axle, as shown in the cad model rendering. Therefore, $l_3 = l_1 = 2\text{ft}$ and $l_4 = 6.5\text{in}$. l_2 is somewhere between $0.5l_1$ and l_1 and θ is in the range $0 - 20^\circ$. Using Equation8.14, Table 8.3.1 is created that relates LHS of Equation8.14 to RHS.

Table 8.3.1: Finding the RHS of Equation8.14 for varying values of θ and l_2

l_2 (ft)	θ ($^\circ$)	mg/P
1	0	-0.541667
1	20	0.175
2	0	-0.270833
2	20	0.08752

As expected, for the low value of theta ($\theta = 0^\circ$), RHS is negative implying stability. When l_2 increases, the system tends to become more stable since the RHS has a lower magnitude. A positive value of RHS does not necessarily imply instability but as the RHS increases in magnitude at some point it will become unstable. Using $\theta = 20^\circ, l_2 = 1$ in Equation8.14 this will happen when the magnitude of pull $P = 5.71429 \times mg$ lbs = 188.571 lbs. Since the applied force is unlikely to reach this magnitude, the system should be stable.

8.4 Analysis 4 - Load Cases For Hitch Tube

An important analysis is to consider load cases for the hitch tube that will attach the bike to the cleaning device and the fastener that would connect the hitch to the device. The cleaning device needs to be dragged by a bike and similar to most bike trailers a hollow circular or tubular long-slender rod made of aluminum is ideal for this. A lot of fasteners are also made from aluminum and thus it is considered to make the fastener pins.

This analysis will focus on a hollow cylindrical cross-section for the hitch and a solid cylindrical cross-section for the fastener. Two loading analyses were considered for both parts to identify an appropriate cross-section to use in the final design. The first analysis is for the case when the user starts from rest and the second one is for when the device hits a rocky/bumpy surface and experiences a vertical shock. Throughout the analysis, it is presumed that the system moves in a straight line. Thus, forces and moments due to turning are not taken into account.

8.4.1 Analysis 4.1 - Acceleration From Rest Load Case

This analysis explores the acceleration case where the user is starting from rest and accelerates to the desired speed of 6 mph (8.8 ft/s) in 3 seconds. This is a fairly representative condition of when the user is starting their up and also when the largest acceleration is happening since this constant speed should be held during use.

Uniaxial tension analysis of the Hitch

The force (F) that is applied to the hitch can be calculated using Newton's Second Law. This force is applied axially on the hitch tube regardless of the angle it makes with the horizontal (θ). This force results in uniaxial tension in the hitch tube. This force is due to the inertia of the system. The hitch rod has a negligible mass in comparison.

$$F = ma \quad (8.17)$$

Analysis 1 determined that the maximum weight of the cleaning device is 33.33 lbf. Using Equation(8.17), this results in a force felt by the hitch of 3.04 lbf. Using the definition of stress:

$$\sigma = \frac{F}{A} \quad (8.18)$$

For Aluminum 6061, yield tensile strength is 276 MPa [21]. According to EngineeringToolbox, a general recommendation for use with reliable materials where loading conditions and environment are not severe is 1.5-2. This loading condition fits well with this assumption. Thus, with an SF of 2, the hitch tube would have to have a cross-sectional area of $1E-7 \text{ m}^2$ [22] in order not to fail. This is smaller than any tubes on the market that would be looked at, so this load condition will not be a limitation.

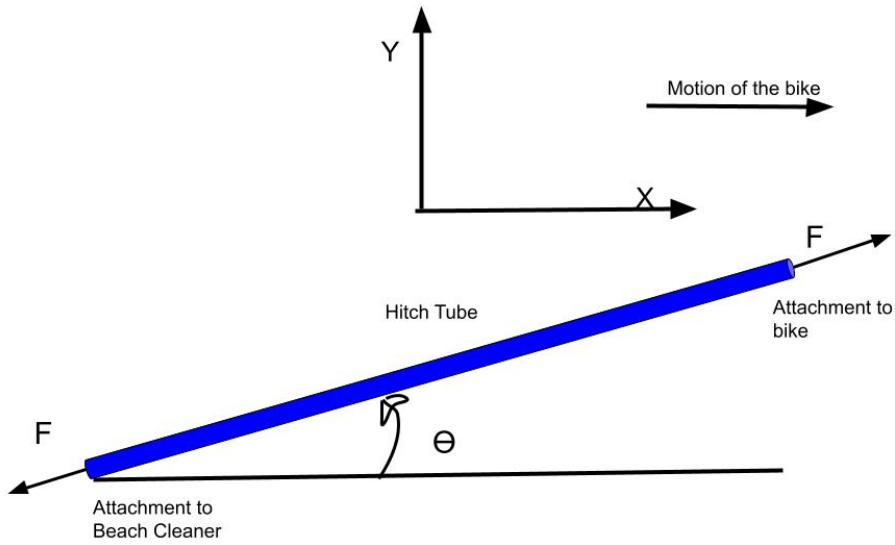


Figure 8.4.1: FBD for the case starting from rest

Shear Analysis of the Fastener

The force F also causes a shear in the fastener that attaches the hitch to the system. Since the fastener cannot support moments in z , only a pure shear is induced on it. If the fastener is made up of Aluminum 6061 it has a shear strength of 207 MPa. The net shearing force is F which induces 2 reaction shearing forces where the fastener pin attaches to the keyhole. Equation 8.19 gives the formula for shearing stress on a circular cross-section where V is the shearing Force which is F , Q is the first moment of inertia, I is the area moment of inertia and t is the thickness of the fastener, R is the radius of the cross-section.

$$\begin{aligned}\tau &= \frac{VQ}{It} \\ \tau_{max} &= \frac{V \left(\frac{4R}{3\pi i} \right) \left(\frac{\pi R^2}{2} \right)}{\left(\frac{\pi r^4}{4} \right) 2r} \\ \tau_{max} &= \frac{4V}{3\pi R^2}\end{aligned}\tag{8.19}$$

Equating Equation 8.19 to the shear strength at failure and solving for the radius, assuming a solid fastener, gives the a of $1.665e-4$ m for the radius.

$$\begin{aligned}\tau_{max} &= \frac{4V}{3\pi R^2} = 207e6 Pa \\ \tau_{max} &= \frac{4 \times 13.52259 N}{3\pi R^2} = 207e6\end{aligned}\tag{8.20}$$

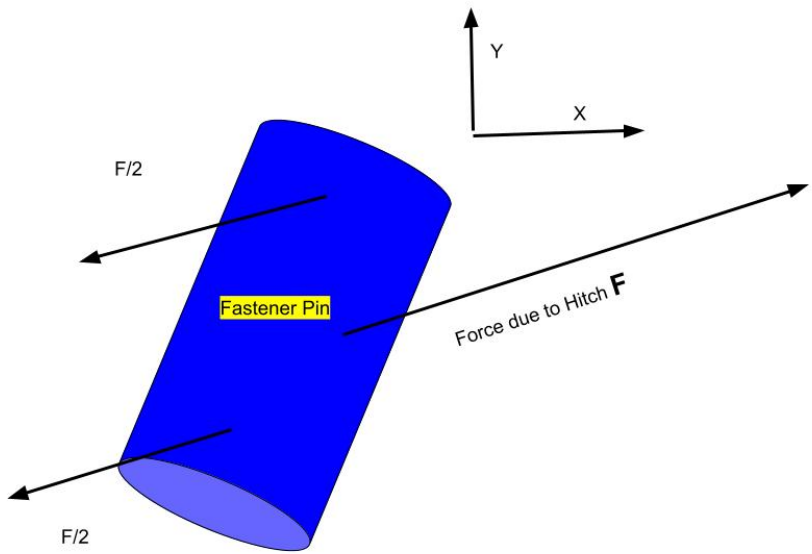


Figure 8.4.2: FBD of the fastner

Even an American size #0 thread diameter is 5 times greater than this. Thus, this force is unlikely to cause sufficient shear and break the fastener. Therefore, the conclusion of this part of the analysis is that both the hitch and the fastener remain intact after the user starts to accelerate and this deliberation will conclude that using the industry standard fastener on a bike is appropriate.

8.4.2 Analysis 4.2 - Vertical Shock Loading

Additionally, a load case was done to account for a vertical shock as the cleaning device hits any rough or bumpy conditions in the sand.

The experiments described in Analysis 1 also were expanded for frequency analysis. This time, a phone was attached welded aluminum plate that was used to collect data. Figure 8.4.5 shows the welded aluminum. Then, a team member ran across the sand court at roughly a constant speed. The constant speed was measured by demarcating the distance and then using a stopwatch to measure time. The initial build-up of speed due to accelerating from rest was taken into account by making the team member run from a point before the point where data collection began. In doing this, data was collected on acceleration vs. time of a plate being dragged across loose sand. This acceleration is vertical to the ground, or in the direction tradition to gravity. This experimental data gives a good reference to how large these shock forces can be.

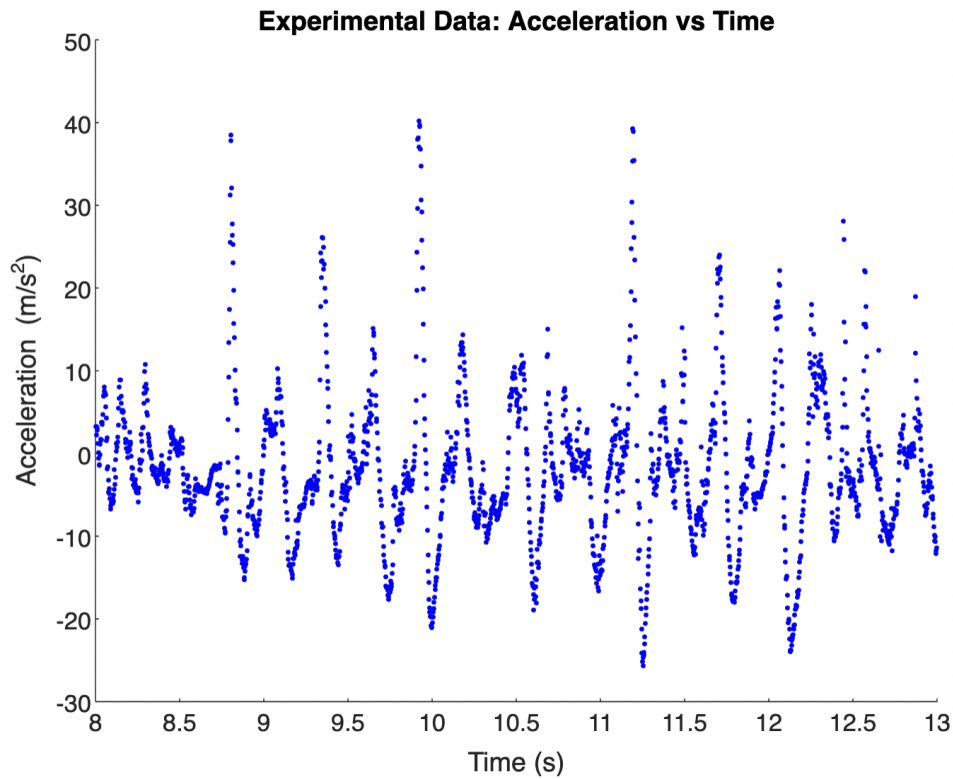


Figure 8.4.3: Load Case 2: Vertical Shock [23]

Along some of the rougher bumps, acceleration reached a little larger than 4G. Therefore, a shock loading of 5G will be used in the analysis for the largest shock that the hitch tube should support.

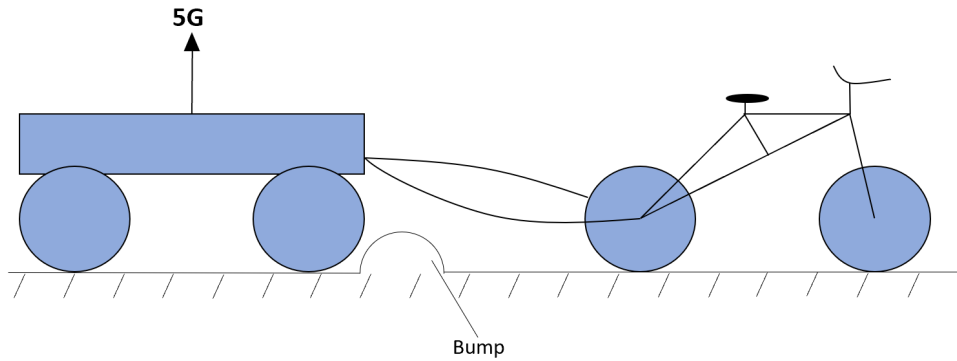


Figure 8.4.4: Bike pulling device and undergoing vertical shock

Figure 8.4.4 is a visualization of the shock force that the cleaning device could experience from the bumps in the sand. A numeric value of the force (F) can be obtained in a similar fashion to the one obtained in analysis 1. Using equations 8.17, where the maximum weight of the cleaning device is 33.33 lbf the value of vertical shock force F comes out to be five times the weight: 166.66 lbf.

This force F causes a shear in the fastener pin that connects the hitch to the system and bending in the hitch, which would be now analyzed.

Shear Analysis of the fastener

This shearing force V of magnitude 166.66lbf (741.34 N) induces shearing stress in the y direction in the fastener. Figure 8.4.5 shows the free-body diagram of the fastener undergoing a vertical shock.

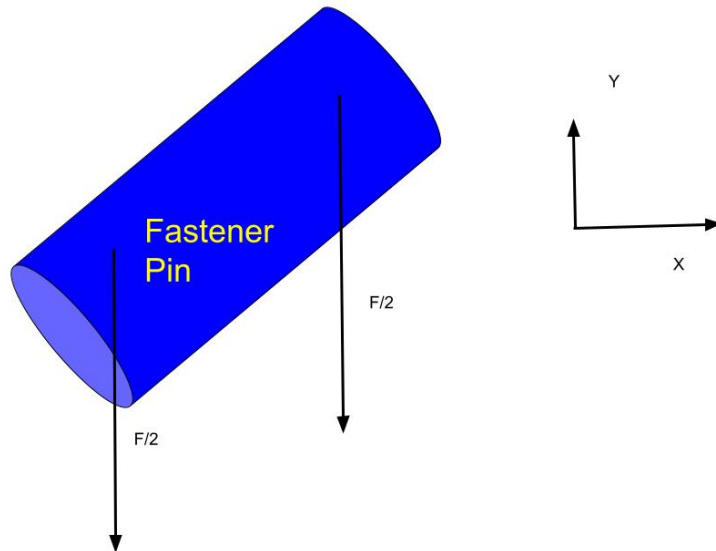


Figure 8.4.5: Fastener with a vertical shock

The max shearing stress can be calculated using Equation 8.19, 8.20 the value for radius R turns out to be 1.233 mm. This value of radius is much greater than the one found in the first part of this analysis. This time, the success of the fastener pin is not guaranteed, since a few types of fastener pins are on the order of 1mm.

Using a safety factor of 2 for the radius to be on the safe side but not increasing the weight by too much, the diameter of the fastener pin comes out to be 4.93149 mm or about 5mm. Thus, to ensure safety a fastener pin of 5mm or larger diameter should be used.

Bending analysis of the Hitch Tube

The force F induces a moment in the hitch tube. The system can be modeled using a fixed-free beam where the fixed side is the bike and the free side is the cleaning device that has just experienced a large force upwards. Even though the hitch is simply supported on both ends, the assumption is that for the impact the beam is effectively cantilevered on the bike side for this analysis. This is because the shock applies a much greater component of force into bending than rotation. The displacement at the device end due to the shock happens so fast that the hitch rod does not rotate. Thus, the beam behaves as if it were cantilevered on the bike side and resists this force. This assumption also places an upper limit on the moment that the hitch rod experiences, since, in reality, the value of the moment will be less than calculated here.

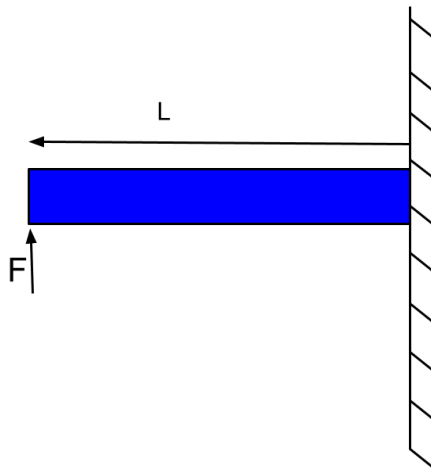


Figure 8.4.6: Free-Fixed Beam Representation

This is a basic Mechanics of Materials problem. The maximum moment is FL . A fair assumption is that the hitch tube will be ≈ 1 meter ≈ 3.33 feet in length which is representative of most bike hitch rods. The maximum stress for this simple beam can be calculated:

$$\sigma_{b,max} = \frac{M_{max} \cdot c}{I} \quad (8.21)$$

Where c is the outer radius of the tube, M_{max} is the maximum moment, and I is the moment of inertia.

$$I = \frac{\pi}{4} \cdot (R^4 - r^4) \quad (8.22)$$

The moment of inertia for a tube can be calculated using Equation(8.22) where R is the outer diameter and r is the inner diameter of the tube.

$$\sigma_{max} = \frac{(166.65 \text{ [lbf]})(3.33 \text{ [ft]})(R)}{\frac{\pi}{4}(R^4 - r^4)} = (275[\text{MPa}])(\text{SF}) \quad (8.23)$$

Combining Equations (8.21) and (8.22), and a safety factor (SF) of 2, a relation of the minimum thickness ($R-r$) can be created for each outer diameter value.

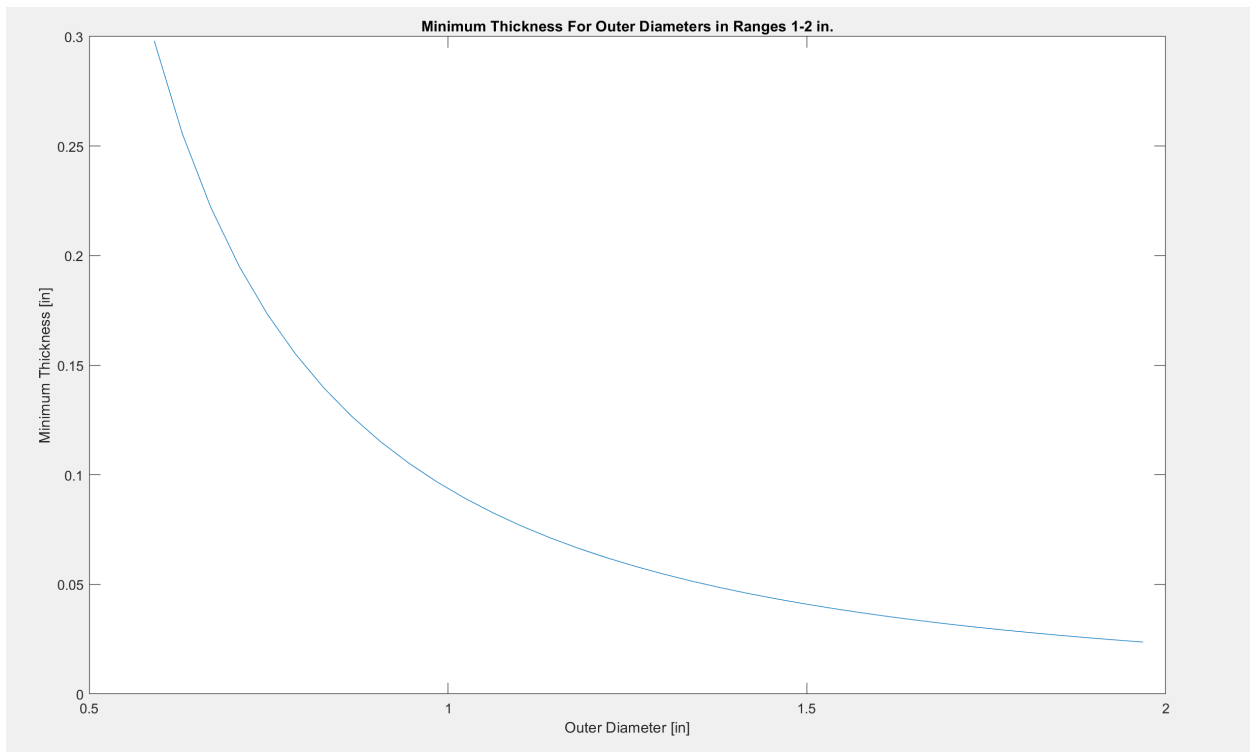


Figure 8.4.7: Plot of Thickness Required for Each Outer Diameter Measurement

The minimum wall thickness required to keep stress under the conditions specified has been plotted above for commonly manufactured outer diameter values between 1 and 2 in..

This can be used when designing a final product by choosing a manufacturer. For example, Vitaneedle, a manufacturing company, has a list of tube dimensions available for sale.

	.020	.022	.028	.035	.049	.058	.065	.083	.095	.096	.120	.125	.156	.188	.250	.313	.375	.500	.625	.750	1.000	1.125	1.250	1.500	2.000
1/8	✓			✓	✓																				
3/16		✓	✓	✓	✓	✓																			
1/4	✓		✓	✓	✓	✓	✓	✓	✓	✓															
5/16	✓		✓	✓	✓	✓	✓	✓	✓	✓															
3/8	✓		✓	✓	✓	✓	✓	✓	✓	✓	✓	✓	✓	✓	✓	✓	✓	✓	✓	✓	✓				
7/16			✓	✓																					
1/2	✓		✓	✓	✓	✓	✓	✓	✓	✓	✓	✓	✓	✓	✓	✓	✓	✓	✓	✓	✓				
9/16			✓	✓																					
5/8	✓		✓	✓	✓	✓	✓	✓	✓	✓	✓	✓	✓	✓	✓	✓	✓	✓	✓	✓	✓	✓	✓	✓	✓
3/4			✓	✓	✓	✓	✓	✓	✓	✓	✓	✓	✓	✓	✓	✓	✓	✓	✓	✓	✓	✓	✓	✓	✓
7/8			✓	✓	✓	✓	✓	✓	✓	✓	✓	✓	✓	✓	✓	✓	✓	✓	✓	✓	✓	✓	✓	✓	✓
1			✓	✓	✓	✓	✓	✓	✓	✓	✓	✓	✓	✓	✓	✓	✓	✓	✓	✓	✓	✓	✓	✓	✓
1-1/8			✓	✓	✓	✓	✓	✓	✓	✓	✓	✓	✓	✓	✓	✓	✓	✓	✓	✓	✓	✓	✓	✓	✓
1-1/4			✓	✓	✓	✓	✓	✓	✓	✓	✓	✓	✓	✓	✓	✓	✓	✓	✓	✓	✓	✓	✓	✓	✓
1-3/8			✓	✓	✓	✓	✓	✓	✓	✓	✓	✓	✓	✓	✓	✓	✓	✓	✓	✓	✓	✓	✓	✓	✓
1-1/2			✓	✓	✓	✓	✓	✓	✓	✓	✓	✓	✓	✓	✓	✓	✓	✓	✓	✓	✓	✓	✓	✓	✓

Figure 8.4.8: Vitaneedle Manufacturer Available Aluminum Tubing [24]

As seen in Figure 8.4.8, along the x-direction the wall thickness is listed in : Along the y-direction, the outer diameter dimensions are listed in inches. The green circles identify available circular tubes for sale. Based on the Figure 8.1.3, which visualizes the minimum thickness for an outer diameter in Figure 8.4.7, the Vitaneedle Manufacturer link was used to determine if the desired aluminum tubing specifications are available for purchase in bulk. A desirable tube is one that can attach to a universal bike hitch, minimized weight but also does not fail, and preferably has a smaller outer diameter so it does not interfere with the wheel. Thus, this analysis determined the aluminum tubing used. The bike attachment that was purchased in prototyping had a diameter of 1 in., so a design including 1.5 in. of outer diameter and thickness of 0.06 is appropriate. From Figure 8.4.8, tubing with an outer diameter of 1.5 in that can be purchased in this thickness is either 0.058 or 0.065 in. thick. Many of the designs seen in trailers have aluminum tubing that connects the trailer to a bike are in this size range, so it is very logical.

8.5 Analysis 5 - First Vibration Mode of a Flat Plate

In order to get the sifting plate to actually sift the sand, one or more vibration modes need to be excited. To get a ballpark of what frequencies need to be excited, the first vibration mode of a flat plate is calculated. But before numbers get put to paper, a couple of assumptions need to be made. First, the relation between stiffness, mass, and cross-sectional area is assumed proportional when the plate becomes perforated. Second, a material assumption is that aluminum will be used. Finally, all edges are assumed to be fixed. From Roarke's Formulas for Stress and Strain the first mode of vibration is given by the 15th row in Table 16.1 within the text [23]. Additionally, the geometry of the holes in the plate is taken into account for a step further in the analysis. The holes are proposed to be a quarter in diameter and hole centers are half of an in apart.

$$f_1 = \frac{K_1}{2\pi} \sqrt{\frac{Dg}{wa^4}}, \quad D = \frac{Et^3}{12(1-\nu^2)} \quad (8.24)$$

Table 8.5.1 contains a breakdown of the variables and their meaning.

Table 8.5.1: Variables contained within Equation(8.24) [23]

f_1	first modal frequency Hz
g	Gravity
a	length of the plate
b	width of the plate
E	Modulus of Elasticity
t	thickness of the plate
ν	Poisson's ratio
K_1	Value from table based on the ratio of plate length and width [23]
w	Uniform distributed pressure over the plate including the weight of the plate

Equation(8.24) can be condensed for a square and simplified a little bit into:

$$f_1 = \frac{K_1}{2\pi} \sqrt{\frac{Ebt^2}{12(1-\nu^2)\rho a^6}} \quad (8.25)$$

Equation(8.25) introduces a quick simplification of mass into ρV which then becomes ρbat where ρ is the material density. Next, the values of the proposed material, Aluminum 6061 are shown in Table8.5.2 [21].

Table 8.5.2: Properties of Aluminum 6061 [21].

ρ	E	ν
2770 kg/m ³	71 GPa	0.33

For the analysis, the plate is assumed to be a 24-by-24-in square with a thickness of 0.0625 in. For a square plate, $K_1 = 36.0$ [23]. All values were converted to metric and

when the calculations were done, the first modal frequency came out to be **35.17 Hz or 221 rad/s**. This value differs significantly from data collected via a phone accelerometer. The values found through testing when using a bike to drag an apparatus through sand can be found in Table 8.5.3.

Table 8.5.3: Experimental Oscillatory Data

Time (s)	Speed (mph)	Weight (lbs)	ω (rad/s)
13.22	3.61	5.07	14.82
18.6	2.566	5.07	15.21
8.82	5.411	5.07	17.81
22.67	2.105	7.2	15.96
14.65	3.258	7.2	16.09
8.06	5.922	7.2	15.71
18.06	2.643	10.01	15.06
16.09	2.966	10.01	16.46
8.31	5.743	10.01	17.1

A few possible ways to get the frequency closer to exciting the first mode of the flat plate is to increase the speed at which someone travels on a bike. These trials were done at around walking pace and if the data were extended proportionally to the target of 6 mph travel speed, the overall estimate for vibrational frequency becomes only marginally closer to the calculated frequency, which means significant changes need to be made in order to reduce the natural frequency of the plate. One possible way the modal frequency of the flat plate can be reduced is by making the plate thinner, although the given thickness analyzed is close to what manufacturers may limit on thicknesses sold. A different material could be used, one that is less stiff with a lower elastic modulus, but corrosion resistance will have to be evaluated as well. Next, changing the boundary conditions to simple supports results in a large reduction of natural frequency. In *Roarke's Formulas for Stress and Strain* the value for K_1 is reduced to 19.7 for a square plate simply supported on all edges [23]. Therefore, the best possible way to excite the first mode is to use simple supports to fix the plate to the device.

8.5.1 Calculations for the Perforated Plate

For the next part in the plate analysis is the consideration of the perforations in the sheet. For that consideration a square pattern of holes is assumed and Equation 8.26 is used [25].

$$\frac{E^*}{E} = 0.5280 + 2.0035\eta - 5.4758\eta^2 + 7.7474\eta^3 - 3.8968\eta^4 \quad (8.26)$$

In Equation 8.26 E^* is the new consideration for the Elastic Modulus and η is the ratio of hole edge distance to hole center distance. Using the hole geometry given in the beginning of the analysis, the new calculation for the first natural frequency of a perforated aluminum plate is **36.81 Hz or 231.3 rad/s**. The addition of holes did not provide a significant change to the natural frequency.

8.5.2 Modal Finite Element Analysis

For an extra measure of validation of calculations a Finite Element Analysis (FEA) was done using Ansys Workbench. The geometry described in the earlier parts of the section for the perforated plate was created in SolidWorks and exported to be used in Workbench. Using the material properties described in Table 8.5.2, shell elements, and applying fixed boundary conditions to the edges of the plate the model the modal analysis was run. The FEA model is shown in Figure 8.5.1 below.

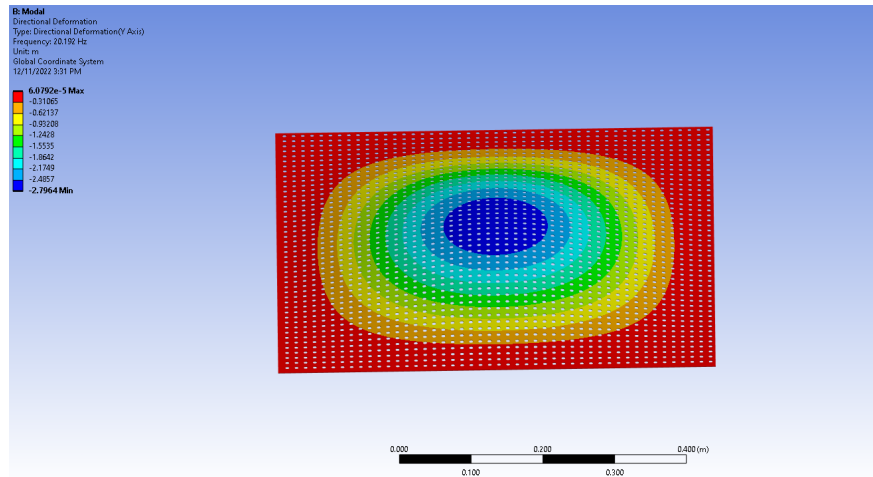


Figure 8.5.1: The First Mode Shape for the Perforated Plate

In the modal analysis the finite element model returned a value of the first natural frequency is **20.14** Hz or **126.6 rad/s**. Interestingly enough, when running the calculations for a simply supported plate ($K_1 = 19.7$) in Equation 8.24, the natural frequencies line up with the FEA model within 0.05 Hz.

8.6 Analysis 6 - Thermal Analysis for Gear Compatibility

Most substances that gears are made up of expand when the temperature changes. This is true of steel, aluminum, carbon and other. For manufacturing purposes the group would be using PLA (Polylactic acid), a thermoplastic monomer with a coefficient of thermal expansion $\alpha = 68 \frac{\mu m}{m - C^\circ}$. PLA is used as it is a commonly available cheap material that is used by most 3D printers, thus allowing the gears to be mass produced. In this analysis, it will be shown that the inner gear and the pinion remain compatible even after they thermally expand. This analysis will analyze compatibility in the radial dimension and along the arc (angular compatibility).

For this analysis, the gear has an inner gear (Gear 1) of pitch diameter 0.0762m (3in) with 30 teeth and a pinion gear (Gear 2) of pitch diameter 0.0381m (1.5in) with 15 teeth. For 2 gears to be compatible they must have the same diametral pitch (DP) which is the ratio of the number of teeth (N) to the pitch diameter(D).

$$\begin{aligned} DP_1 &= \frac{N_1}{D_1} = 30/0.0762 = 393.701 \\ DP_2 &= \frac{N_2}{D_2} = 15/0.0381 = 393.701 \\ DP_1 &= DP_2 \end{aligned} \tag{8.27}$$

Therefore, the two gears are initially compatible at room temperature of $27^\circ C$. According to the sand on the beach can be as much as 150F which is roughly $67^\circ C$ [26]. Thus there is a temperature change of 40 K. For the purposes of this analysis, the gears are approximated as circles with their pitch diameter being the circle's diameter. The only source of heat that is considered is that from the sand, thus heat due to the motion of the gears and friction is ignored. This assumption could be made since the mechanism is not rotating at high angular velocities.

8.6.1 Radial Compatibility

The change in radius of the gear is given in Equation 8.28 where R is the initial radius, α is the coefficient of linear thermal expansion, ΔT is the temperature change.

$$\Delta R = R\alpha\Delta T \tag{8.28}$$

For the dimensions specified, the temperature change and the value of α given, this comes out to be $103.63 \mu m$ for the inner gear and $51.816 \mu m$ for the pinion gear. This is an inconsequential change in the pitch diameter. The change in pitch diameter is smaller than the tolerances under which most gears are manufactured and thus if the 2 gears were produced such that they are in radial contact at room temperature, then they will be in radial contact after expansion.

8.6.2 Angular Compatibility

The angle between any 2 consecutive teeth is given by Equation 8.29 where N is the number of teeth.

$$\theta = 2\pi/N \quad (8.29)$$

This comes out to be 0.20944 rad for the inner gear and 0.419 rad for the pinion gear.

The arc length separation (Δarc) between 2 consecutive teeth is just the product of the radius and the angular separation θ and the change in arc length is given by Equation 8.30

$$\Delta arc = \Delta R\theta + R\Delta\theta = \Delta R\theta \quad (8.30)$$

Since the gear is circularly symmetric, θ does not change and consequently $\Delta\theta = 0$. ΔR was calculated using (8.28). Thus the change in arc length is $\approx 21.71090 \mu m$ for both inner and pinion gear.

It is surprising to see that the change in arc length is the same for both gears. This implies that the arc length separation between the gears does not change regardless of what temperature they are brought to, as long as they are made up of the same material.

This is shown in Equation (8.31)

$$\begin{aligned} \Delta arc_1 &= \Delta R_1\theta_1 = \frac{2\pi}{N}R_1\alpha\Delta T \\ \frac{\pi\alpha\Delta T}{DP_1} &= \frac{\pi\alpha\Delta T}{DP_2} \end{aligned} \quad (8.31)$$

$$\Delta R_2\theta_2 = \Delta arc_2$$

$$\Delta arc_1 = \Delta arc_2$$

Therefore, if the gears were initially had a compatible arc length separation, then they will continue to have a compatible arc length separation after expansion.

In conclusion, the gears are guaranteed to have angular compatibility regardless of temperature provided they are made of the same material and were compatible, to begin with. However, the gears may not be radially compatible at high temperatures but that is not an issue since the change in temperature is not too high and thus the expansion is small enough to be ignored. Finally, if the gears were made using steel or aluminium then the radial separation after expansion would be even smaller as $\alpha_{steel} \approx \alpha_{aluminium} < \alpha_{PLA}$.

8.7 Analysis 7 - Shear Analysis of Axle

A point of failure for the entire mechanism is the axle of the brush. The axle is moving at a high angular velocity and if encounters heavy (infinitely heavy for the analysis) debris, then the bristle that hit it would come to instantaneous rest. This would generate a shock through the bristle which then passes through the axle since the rest of the bristles are still rotating. This may cause either the bristle to fail in bending or the axle to fail in shear due to the reaction torque being applied by the bending of the bristles. The failure of the individual bristle is not a matter of concern however, the failure of the axle is a matter of grave concern and is thus discussed here.

Material and Physical Properties of Nylon Bristles:

- $E = 2.7\text{GPa}$
- $L = 0.1571625\text{m (}6.1875\text{in)}$
- $d = 0.635\text{mm (}0.025\text{in)}$

Material and Physical Properties of aluminium Axle:

- $D = 0.015875\text{m (}5/8\text{in)}$
- $\tau_{st} = 207\text{MPa}$

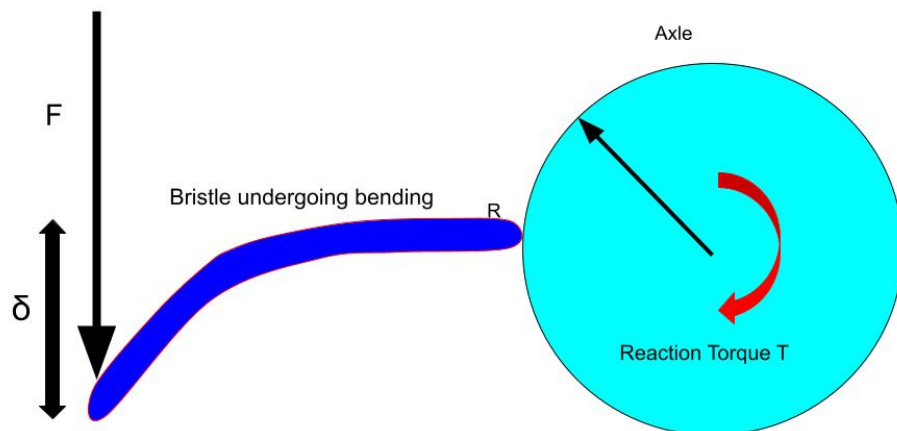


Figure 8.7.1: Mechanics of the collision

Figure 8.7.1 describes the mechanics of the collision. A long bristle of length L undergoes bending due to collision with debris. This collision induces a reaction torque T which induces a torsional shear in the axle. For the purposes of this analysis, the bristles are assumed to be long and thin cylinders that are cantilevered to the axle. Thus, the bristle is modeled as a cantilevered beam undergoing bending. The mass of the bristles is negligible in comparison with the axle and the inertia of the bristles is negligible compared to the axle. The effect of gravity is ignored. The brush is modeled as lines of bristles, with individual bristles in line.

The first step in this analysis is to find out the force applied on the bristle that would cause the axle to break in shear. As Figure 8.7.1 indicates the collision with the debris induces a force (F) on the bristle which induces a reaction torque (T) in the axle. The value of this torque and consequently the Force can be found by considering the worst-case scenario, which is the torsional shear that the axle can support before failure, as shown in Equation 8.32.

$$\begin{aligned}\tau_{max} &= \frac{TR}{J} = \frac{TR}{\frac{\pi}{2}R^4} = \frac{2T}{\pi R^3} \\ \tau_{max} \pi R^3 / 2 &= 162.61 \text{ Nm} \\ F &= T/(R + L) = 984.9 \text{ N}\end{aligned}\tag{8.32}$$

The next step in the analysis is to find out the force on the bristle that causes it to deflect downwards by 1cm. The value of 1cm is chosen because in the group's experience with the prototype the bristles did not deflect more than 1cm. A deflection of more than 1cm induces a permanent bend in the bristle, thus increasing the probability that it will fail in the next interaction.

$$\delta_{tip} = \frac{F_b L^3}{3EI} = 0.01 \implies F_b = \frac{3\delta_{tip} EI}{L^3} = 1.6653e - 4 \text{ N}\tag{8.33}$$

The value of the force depends linearly on δ_{tip} . Thus, if the actual deflection was 1/10 the assumed deflection, then the force would be 1/10 as well.

Figure 8.7.2 shows the design of the brush. A number of bristles are arranged in a single line. In an actual brush, there will be multiple such lines.

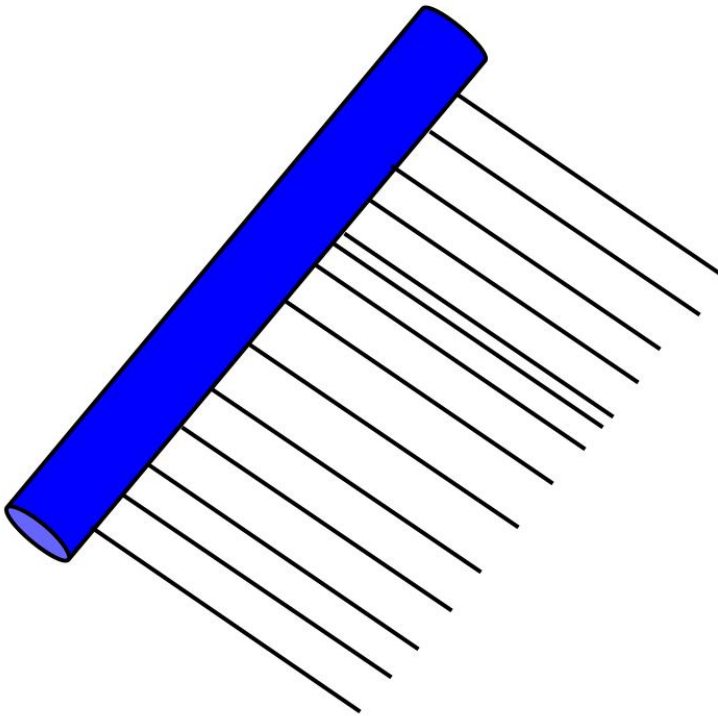


Figure 8.7.2: Model of the brush: A single line of bristle

The brush is assumed to be a linear sequence of such bristles, thus the force applied on n such bristles would be $n * F_b$. This combined force may be enough to cause a shear in the axle if the net force equals or exceeds the force calculated using Equation 8.32.

$$nF_b \geq F \implies n \geq 5914736.026 \quad (8.34)$$

Thus, about 6 million bristles would have to deflect by 1cm while not breaking to shear the axle. If the deflection had been 10cm, then about 600 thousand bristles would be required since the force F_b scales linearly.

Since the design does not have 600 thousand bristles on the brush, the conclusion of this analysis is that the axle is not likely to fail in shear.

9 Final Design

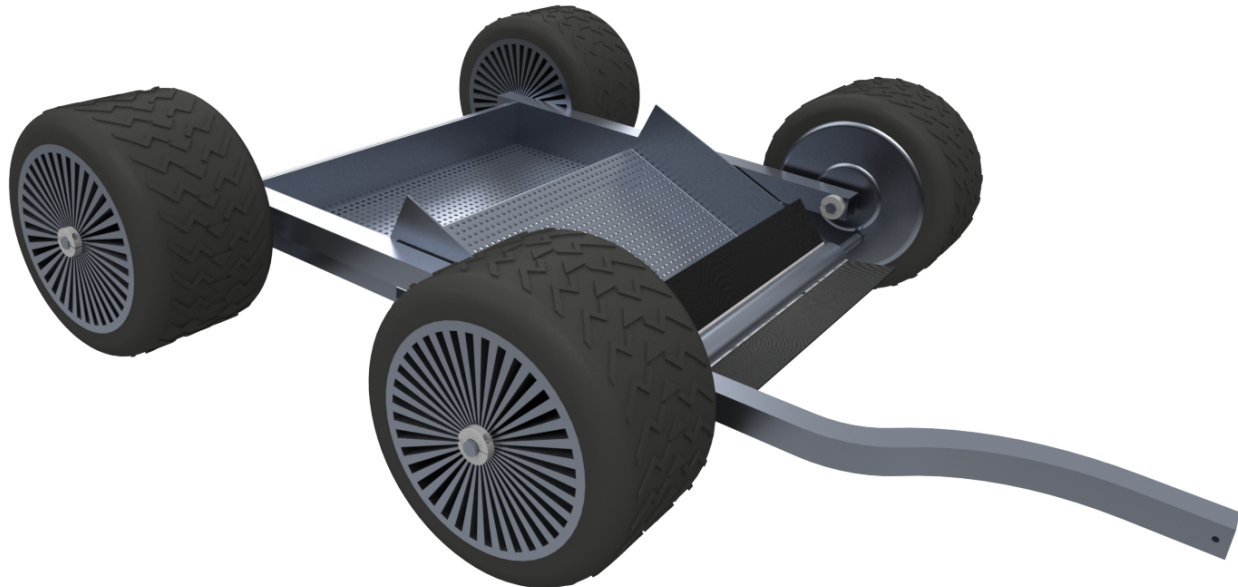


Figure 9.0.1: Rendered Design for Beach Cleaner

Figure 9.0.1 shows the rendering of the final CAD model that the team came up with. The final design consists of 4 equal wheels, with the front wheels having an inner gear-pinion mechanism, a ramp and a sifter, a body of aluminum tubing, a front axle with bristles, a back axle and a handle that attaches to the bike.

The wheels are all 13in diameter and 7.5in wide. The back wheels are purchased parts and their dimensions can be found in the drawings. The front wheels consist of a tire, a rim and a cover with a hole. The cover and rim are 9in. in diameter and the cover is about 1/4in. wide. The wheel rim is fixed to the tire and an inner gear is attached internally to the rim that rotates with it.

The cover is attached to the aluminum tubing chassis through an axle that it is centered upon. The cover contains a key-shaped hole that through which the brush axle passes. Finally, the brush axle that passes through the cover gets fixed on the rim through a bearing. The pinion gear is attached to this axle.

The inner gear is twice the pitch diameter of the pinion gear which has a pitch diameter of 64mm.

The next part of the design is the brush. The brush consists of an axle that has a two-in thick diameter in the middle and a (5/8) in diameter at the ends and is 30.5in long. The axle also contains T-shaped notches for bristle retainers to slip through.

The sifter and the ramp are perforated sheets that are sheet metal bent. The sifter is 23.45in wide and 9.88in long. The sifter is attached to the chassis using an L-shaped bracket.

The chassis of the device is made up of square aluminum tubing of cross-sectional area $0.17in^2$, with the outer side length being 1.5in and the inner length being 1.44in.

Finally, the back axle is simply a rod of diameter (5/8)in and length 44in.

10 Manufacturing Considerations

10.1 Main Frame

The frame can be made of Aluminum 6061-T6. Al606-T6 has a relatively high strength, is easily welded, and is widely used for making bicycle frames (which is of similar function to the frame) [27]. The T6 refers to the temper or degree of hardness, which is achieved by precipitation hardening. This grade has a good strength-to-weight ratio and is also heat-treatable. With great formability and weldability, The primary elements on the chassis are the one L-bracket and the square aluminum tubing. The square tubing is the primary source of rigidity of the chassis while the L-brackets will hold the perforated sheets in place and provide a sort of "backboard" for the trash to be collected instead of being thrown over. The square tubing can be cut to the correct lengths and the holes to fit the axle can be done using a drill press. The L-brackets can be made from a single L-bracket of the total length needed and formed into the appropriate horseshoe-like shape by cutting a 45-45-90 triangle with the 90° vertices in the locations that must be bent. The cutout allows the top portion of the L-bracket to be bent with the edges where the material was removed on the bottom portion to meet and be welded together at the bisecting line of the new corner. Then, the L-brackets can be welded alongside the top faces of the frame with the top faces flush and this would complete this sub-assembly. Figure 10.1.1 shows how the two components are mated together to create the frame.



Figure 10.1.1: L-Bracket and Square Tubing Mated Together to Form the Chassis

10.2 Sifter and Ramp

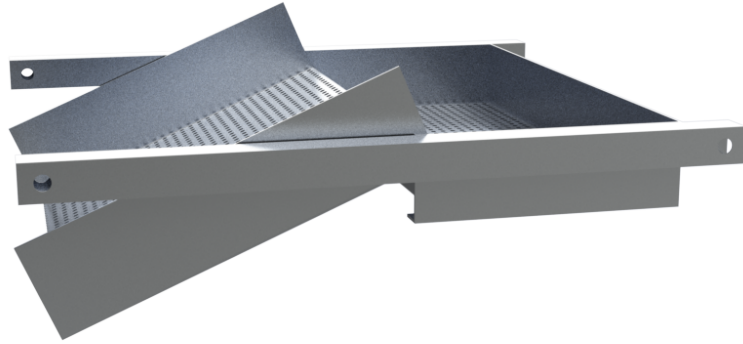


Figure 10.2.1: The Sifter and Ramp Sheet Attached to the Frame

Figure 10.2.1 shows the design of the sifter and ramp attached to the frame. The sifter and ramp are made up of Aluminium 6061-T6 which has a thickness of 0.06in. Aluminum 6061-T6 has various desirable properties such as low density (2700 Kg/m^3) which corresponds to a light mechanism, and high ductility with a flexural strength of (300 MPa) [28]. Aluminum 6061-T6 has a high machinability of 50% which is high compared to other kinds of Aluminum like Aluminum 1100 - O (10%) but lower than Aluminum 2024-T3 (70%). However, Aluminum 2024-T3 is much less corrosive resistant which is of paramount concern since the design would be used on a beach. Furthermore, sheets of aluminum 6061-T6 are readily available and cheap to procure. The sifter and ramp could be made out of a large sheet of Aluminum 6061-T6 which should be bought and cut in accordance with the shape shown in drawing BC 10.2.2 on the next page. This can be achieved using a plasma cutter or a press cutter. Holes in the sifter can be stamped either before or after the sheets are cut to size. The next step is to bend the aluminum sheet to form the ramp at an angle of 120° . A common manufacturing process for this is called sheet metal bending which is accomplished using a brake.

Alternatively, the various sheets of the sifter ramp assembly could be cut and then joined together by creating edge-welded joints.

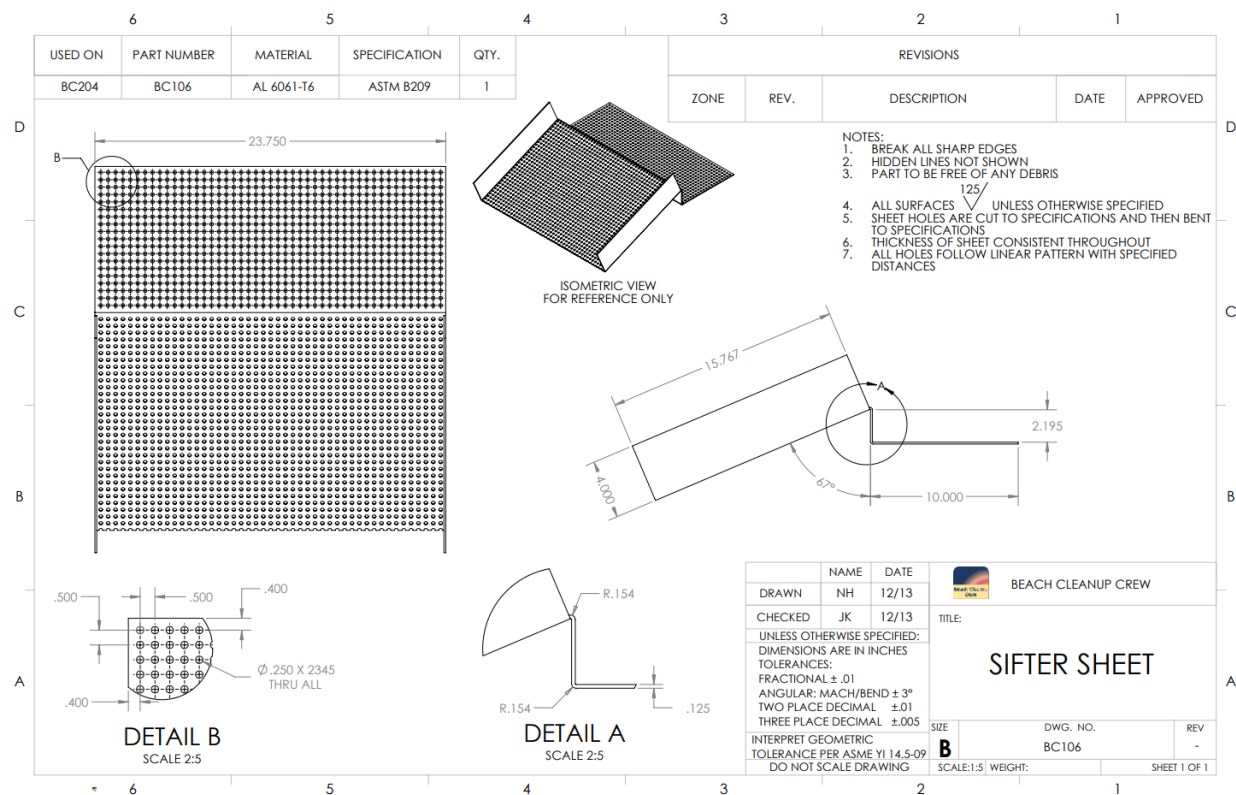


Figure 10.2.2: blackprint Drawing of the Sifting Sheet

10.3 Wheels

10.3.1 Back Wheels

The Back wheels can simply be purchased online. Looking at the market, there is a plethora of sand wheels available within the dimensions the design requires. Any wheel that is 13 in. in diameter would work. As for thickness, as long as the wheel is sand friendly that is fine - but 7.5in to conform with the front wheel would be ideal. From experience, the majority of axles for small-to-medium-sized wheels have an axle diameter of 5/8in, so that is what was designed for. In practicality, any wheel that has a 13in diameter and is compatible with a 5/8in axle would work fine. The VEVOR Beach tires sold on Amazon fit perfectly with the specifications [29].

10.3.2 Front Wheel

The front wheel is comprised of the following parts: **tire** that contacts the ground, a **cover** that attaches to the chassis and is stationary with an off-center hole through which the brush axle passes, a **rim** that attaches to the tire and the dead axle through a bearing that allows the tire and rim to rotate but keeps the dead axle stationary, an **inner gear** that is mounted on the rim and rotates with the tire, a **pinion gear** that is compatible with the inner gear is mounted on the brush axle and transmits the tire rotation to the brush.

Bearings: 2x on each wheel (Product Link: McMaster-Carr). Permanently lubricated ball bearings offer protection from the outside environment such as sand. Experience with the reel mower that was used in testing also proved the importance of a covered ball bearing because a single session of light work on sand caused crunching noises from the normal bearings. Bearings specified as permanently lubricated (covered from the outside) R10 bearings to fit 5/8 in the axle. Can shrink-fit to fit bearings into the front wheel.

As for the pinion mechanism. The outer gear should be milled into the front wheel. Then, the metal gear pinion can be purchased online. These types of gears are readily available from McMaster-Carr. The internal gear used in this design have a 20° pressure angle and should ideally be made of the same material as the rim of the front wheel because Analysis 6 found there was thermal analysis compatibility that allowed no residual stress this way, but for the sake of corrosive resistivity it is not the best option. The inner and pinion gears provide a gear ratio of 3 with the pinion gear having a keyhole and an inner diameter of 5/8in would work. The tire should also be purchased. A tire with a diameter of 13in would work for the design.

The rim and the cover are manufactured by the team. Both parts should be cast out of Al A380. Al A380 is the most popular aluminum available for casting. Although any kind of casting would suffice, sand casting should be performed due to its simplicity. The casted parts should then be surfaced. Ideally, the tire would simply slide on top of the rim by hand and the cover would fit. Finally, a hole in the cover should be drilled with a drill bit that would be 5/8in to match the axle diameter. The axle and the hole should fit in tightly. To attach the inner gear to the casted rim, a TIG weld should be created on the outside of the inner gear that encompasses the gear without gaps for stability.



Figure 10.3.1: Rim (left) and Cover (Right)

10.4 Bristles

Most commercial-grade bristles are made of two common synthetic polymers: Nylon or Polyester. Manufactured bristles are commonly available and most likely not worth producing since they can be bought by the foot at mass. For the design either polymer would be fine. Per MatWeb, both materials have a similar Young's Modulus: Nylon 6, cast (1.3-4.2 GPa) and Thermoset Polyester, Rigid (1-10.6 GPa) and similar Flexural Strength: Nylon 6, cast (20.0 - 150 MPa) vs Thermoset Polyester Rigid(53.8 - 265 MPa). Analysis 8.7 for Nylon bristles would apply to the polyester bristles as well thus the bristles should not be a point of failure.

With the calculations from the analysis, most synthetic bristles are made of Nylon 6, cast as it is a readily available cheap material. One such seller is Precision Brush [30] which sells Nylon brushes in 4 different diameters: 0.006in, 0.010in, 0.018in, and 0.025in. To justify using 0.025in, The team used Equation 8.33. Because a larger diameter of brush results in a larger moment of inertia, the larger bristle size will result in the smallest deflection (δ_{tip}). A smaller tip deflection means that the bristle is less likely to break. The analysis also shows that the force applied by the bristle, even hundreds of thousands of bristles is not enough to shear the axle. Thus, a wider bristle is preferred.

The length of the bristle should be so chosen that in combination with the axle and roller the total diameter of the brush matches the diameter of the wheels. This would ensure that the brush, centered at the same height as the wheels, touches the ground without going underground. This, along with a gear Ratio of 3 would impart enough energy into the debris to fling it over the ramp as shown in Analysis 8.2.

10.4.1 Attachment to Roller



Figure 10.4.1: Commonly available Nylon bristles

Most commercially sold bristles are stacked on top of a T-shaped slider, called a retainer, as shown in figure 10.4.2. Thus the roller needs to have an appropriate notch into which the brush can slide through. The brush can be fixed to the roller with an epoxy resin.

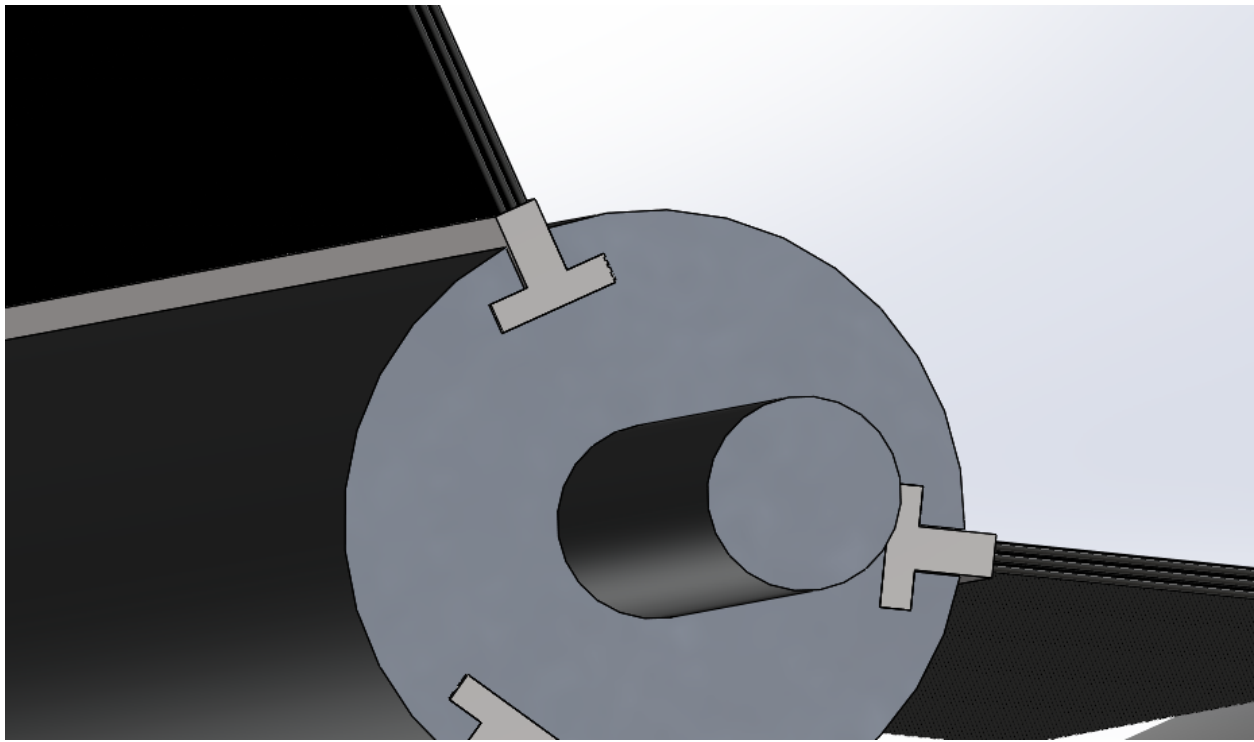


Figure 10.4.2: T-Shaped Slot with Brush Attached

The design for the roller is the particular shape for the notch that the slider would slip in as shown in 10.4.2. If a retainer with bristles shown in 10.4.1 is not available then the notch in the roller will be redesigned such that the available retainer slides into the notch. The number of notches in the roller determines the number of lines of bristles that can be attached. For this design, there are 3 notches spaced 120° apart.

10.5 Front Axle and Roller



Figure 10.5.1: Design of the axle and roller

For the purposes of the design, the front axle and the roller are considered as a single part and are manufactured together. The front axle and roller are made from aluminum 6061-T6, which is very commonly available cheap aluminum that has a 50% machinability rating (one of the highest among the types of aluminum that were researched) while also maintaining high corrosion resistance. Also, aluminum 6061-T6 has a high yield strength (276 MPa) [31], which is only slightly less than that of steel (350 MPa). However, the density of aluminum 6061-T6 (2700 Kg/m^3) is significantly less than that of steel ($7800 - 8000 \text{ Kg/m}^3$) [32]. Since weight is of particular concern to the design, Aluminum 6061-T6 is preferable.

The diameter of the axle of the part that goes through the wheel is $5/8$ in. This is because this is such a universal diameter size of most of the wheels commercially available that the team considers it a standard to comply with. The machine this part, start with a larger diameter rod, the size of the roller, and lathe it down to $5/8$ (except a small portion that will be milled to fit a key that can fit into the pinion's keyway). The key will be a square sunk key, which will include a taper for a tight fit.

To make the T -slot retainer start by milling a central path that corresponds to the vertical length of the retainer. Then using a woodruff keyseat cutter, mill the horizontal section of the cut. An example of a keyseat cutter is shown in Figure 10.5.2. Repeat twice to make the other 2 retainers. Finally, mill the ends of the axle to create the keyseats to hold the key for the pinion gear, removing the rotation degree of freedom between those components.



Figure 10.5.2: Woodruff Keyseat cutter

10.6 Back Axle

The back axle will be a standard axle with no additions. For this reason, the axle will be purchased for simplicity. An important consideration for aluminum axles is fatigue and the ability to hold high stress because of the bumps in the sand constantly being hit. Al 7075 alloy series is the one that offers the most strength, low density, great machinability, fatigue loading, and great resistance to corrosion. It is an appealing candidate for stressed structural parts.

11 Prototype

The manufacturing of the prototype was far from the ideal manufacturing of the design discussed throughout this report. Instead of buying and having to deal with different materials between gears and other components (terrible for anything that was meant to be solidly connected as different metals should not be welded together), it was decided from the start that the gear system from an old, thrown-away reel mower would be salvaged and used within the prototype. This was good for the previously stated issue but ended up causing quite a bit of issues down the line.

The inner gear was molded into the wheels that came from the used reel mower. These wheels were small and not sand friendly, and therefore the wheel was epoxied to a bigger, thicker wheel with treading. Of course, this is far from the ideal case where the front wheel is manufactured. This, however, prevented the team from the hassle of self-creating the wheel composed of a rim, a cover and a tire. Another byproduct of this was that using the reel mower's wheel covers and pinion gears was now a requirement. This meant modifying other bought/made parts to attach properly. Two holes were drilled in specific spots of the frame in order for the frame to attach as flatly as possible to the wheel cover.

The head of the brush axle that went into the pinion gear had to be reduced in size since the 5/8in axle rod did not fit inside the pinion which had a diameter of 1/2in. To do this, the axle reduction was cut off the reel mower and then both those parts and each end of the brush axle were given a new, flat surface where a hole was then drilled. A much smaller rod was then cut to size to fit in the drilled holes, between the axle and the reduced part, centering them with each other. This process prepped them to be welded. Finally, the modified axle was able to fit into the pinion gears properly.



Figure 11.0.1: In-progress Prototype

The frame was the next assembly needing to be built. This was done by first purchasing and cutting the square Al 6061 tubing and L-brackets to size. These were then assembled in a way that fit the modified axle and then TIG welded together. The frame and wheels are assembled as shown in Figure 11.0.1. Now, the perforated sheets needed to be bent into shape on the sheet metal brake and fastened on. The original plan was to weld, but with the metal sheets that were bought being 304 stainless and the L-brackets they were meant to attach to being Al 6061, welding was out of the picture. Thus, holes were drilled in the L-brackets and small bolts/nuts were used to fasten the sheets to the frame.

The final assembling of the prototype, as seen in Figure11.0.2 was relatively easy compared to the rest of the process, just consisting of putting axles through holes and bolting things down, etc. In the end, the team was happy with how the prototype turned out, but there were obvious things that should be improved upon in the final manufacturing of the design.



Figure 11.0.2: Finished Prototype

The cost of the final prototype came out to roughly \$292, which was below the \$400 budget given to each group.

12 Conclusion

12.1 Lessons from Design

As with every design, first, second, third, etc. drafts are not perfect and it takes many more iterations for everything to work out properly. With the pace of this course, the teams' designs were clearly imperfect or improbable from the start. The connecting bar for connecting the beach cleaner to a bike is a good example of a part that was left on the back burner as a less important aspect of the design. That is easily seen in the prototype as well as the CAD of the beach cleaner.

The front axle was designed to have a key that would fit in the pinion keyhole. This feature updated the hole in the cover to accommodate the key. This means that the system is no longer weatherproof. Thus sand will enter the system and would render the device useless with time. In reality, the key is a separate part that would sit in a recessed keyseat cut into the axle, therefore creating an assembly that does not violate the integrity of the weather-proofing. With it designed this way instead, the cover would be put on the axle before the key is put into the keyseat recess.

Ideally, the sifter and the ramp would have included a collection area that makes it easy for the trash to be picked up and disposed of when full, say it went into a bag that detaches. As it stands, the garbage would, in the best-case scenario, pile on top of the sifter and the user would have to manually remove the trash. This is an obvious area to improve upon, mostly consisting of adding something that collects the trash better, not letting lighter pieces of trash fly over the basket, and something to allow the user to dispose of the trash easily. Thus, making the sifter and the ramp would be made as two separate parts with the sifter being detachable or an attachment for a garbage bag being provided.

12.2 Lessons from Prototype

It was decided after seeing the prototype work that the gear ratio was too high which lead to debris being flung over the collection area and back onto the ground. The prototype had a gear ratio of 5. Since energy is proportional to ω^2 , too much energy was imparted onto the trash. The device is also designed for a gear ratio of 2 which would impart 4/25 or about a fifth of the energy that the prototype imparted. However, some debris would still be flung over the sifter and thus the design would need to accommodate some type of "backboard" to help corral the trash that flies by.

The other lesson from the prototype was that the length of the collecting brush was too small. This was incorporated into the final design by making the brush much longer and thus allowing for much more trash to be collected. This consequently increased the size of the sifter.

12.3 Evaluation of Design Criterion

Weight was the most important criterion and the final design showcases that. Most parts are made of lightweight aluminum. The wheels have an extremely large surface area that minimizes the pressure that the device exerts and consequently the device sinks only a little bit into the ground. Thus the effect of drag force, which would have played a major part if the device had sunk significantly into the ground, is minimized. The brush only barely touches the ground, while the ramp does not. Both these considerations make it so that the interactions with the ground are minimized and thus the effect of frictional forces is lessened.

The device also performs extremely well on complexity. In fact, it was designed to be the least complex as possible. This is showcased by the fact that the brush is spun by a gear mechanism instead of an electrically powered one, which eliminated the complexities that electronics present. Furthermore, the design lacks a roof which would have improved the design so that the debris that was flung would have been caught. However, the effect of including a roof would have meant more analysis at least to make the system aerodynamic, since the roof would have induced significant drag forces. The device also contains a welded sifter and ramp instead of a detachable one. A detachable sifter would have required more work.

Since the ramp no longer goes inside the ground, the device is not capable of picking up underground trash. This makes the device less efficient since one of the components of efficiency was the ability to collect varying kinds of trash. That being said, the device is capable of collecting plastics, bottles, paper, twigs, etc as long as they are on the surface of the beach. The other component of efficiency was speed. This seems to be well fulfilled as the low weight of the system implies that the system is fast in its movement.

The device is somewhat optimized for cost. The materials chosen for the mainframe, front rim, and brush are some form of aluminum which is cheap and sturdy. However, the system also includes plenty of purchased parts such as the back wheels and the gears. The price of these parts is something that is not in the hands of the team and the overall cost is variable.

The final evaluation criterion was ergonomics. This is where the device performs the worst. As previously mentioned the device is not detachable, does not have a roof and required the user to empty the trash manually. Furthermore, the device is not capable of turning since the wheels do not rotate. Ergonomics was the least important category and is certainly reflected in the overall design.

12.4 Future Design Iterations

When considering the strengths and weaknesses of the design it is again important to remember that designs and prototypes are iterative. Some important aspects were brought up in the previous section and to condense the ideas into a short summary the following changes would improve the Beach Cleaner.

Design the system to be more ergonomic. This would indeed increase complexity for the engineers but the goal of the project is to make the device as easy to use for the customers.

This could include things like a detachable sifter or an attachment for the garbage bag. Making the device capable of rotating with the bike around the turns would also be a major improvement. Finally, the inclusion of a roof would mean that the device would be much more efficient in retaining the debris it collected.

Same materials for any two parts being welded together. In some cases on the design (because of bought parts), the materials are different between parts that seem should be welded. This is not good as different materials do not weld together very well. This was especially an issue during the manufacturing of the prototype where parts such as the perforated sheets were 304 stainless and the L-brackets were Al 6061 and had to be fastened with small bolts instead of welded. Wherever possible (especially if the parts are meant to be welded together), the same material should be used.

One more idea in the design iteration would be changing the location of the brush. In the design, it could not be fixed to the frame due to interference with the bike connection. In a future design, the brush axle could be moved to sit behind the wheel axles which would eliminate the interference issues.

Through all challenges faced, the team learned a lot about the engineering process and would like to continue on environmentally impactful projects. The Beach Cleanup Crew created a successful prototype and design, with which the world can become a cleaner place, one beach at a time.

References

- [1] “Waste items found along beaches in the u.s. 2020,” *statistica*, Standard, 2022.
- [2] P. Arora-Desai. “Plastic pollution: A crisis in mumbai’s beaches and the arabian sea.” (Nov. 13, 2021), [Online]. Available: <https://www.hindustantimes.com/cities/mumbai-news/plastic-pollution-a-crisis-in-mumbai-s-beaches-and-the-arabian-sea-101636309809709.html>.
- [3] “Ballance, a., ryan, p. g., turpie, j. k. (2000). how much is a clean beach worth? the impact of litter on beach users in the cape peninsula, south africa. *south african journal of science*, 96(5), 210-213,”
- [4] H. S. Barber. “Sand man: Walk behind beach cleaner.” (2014), [Online]. Available: <https://www.hbarber.com/sand-sifting-machines/sand-man/>.
- [5] “Bikes at work.” (2006), [Online]. Available: <https://www.bikesatwork.com/blog/how-much-weight-can-a-bicycle-carry>.
- [6] “The engineering toolbox: Rolling resistance.” (2008), [Online]. Available: https://www.engineeringtoolbox.com/rolling-friction-resistance-d_1303.html.
- [7] J. R. Davis, *Corrosion of Aluminum and Aluminum Alloys*. ASM International, 1999, ISBN: 9781615032389. [Online]. Available: <http://ebookcentral.proquest.com/lib/wisc/detail.action?docID=3002410>.
- [8] “An ordinance establishing the fort myers beach, beach and dune management ordinance,” no. 00-10, Jun. 19, 2000. [Online]. Available: <https://www.fortmyersbeachfl.gov/DocumentCenter/View/510/00-10-Dune-Management>.
- [9] “Fat bike tyre pressures – everything you need to know,” [Online]. Available: <https://cambiobikes.com/blog-post/fat-bike-tyre-pressures/#:~:text=10%5C%20PSI%5C%20is%5C%20a%5C%20good,from%5C%20sinking%5C%20into%5C%20the%5C%20snow..>
- [10] H. S. Barber, ““tine raking device”, us 2007/0119606 a1,” Mar. 24, 2009. [Online]. Available: <https://www.lens.org/lens/patent/024-127-499-401-566/frontpage?l=en>.
- [11] H. S. Barber, “Specifications - surf rake,” 2014. [Online]. Available: <https://www.hbarber.com/beach-cleaning-machines/surf-rake/specifications/>.
- [12] “Delfino - walk behind sand cleaning machine.” (), [Online]. Available: <https://www.environmental-expert.com/products/delfino-walk-behind-sand-cleaning-machine-647132>.
- [13] C. Inc., “Sandragin,” 2019. [Online]. Available: <https://www.cleansands.com/sand-cleaning-tool.html>.
- [14] H. A. Lindau, ““sand cleaning tool”, us10280577b1,” May 7, 2019. [Online]. Available: <https://patents.google.com/patent/US10280577B1/en>.

-
- [15] “Environmental engineering considerations and laboratory tests,” United States Department of Defense, Standard.
 - [16] “Welding, tungsten arc, inert gas,” Society of Automotive Engineers, Standard, Sep. 2017.
 - [17] “Unified inch screw threads,” American Society of Mechanical Engineers, Standard, 2019.
 - [18] M. E. P. Francesco Costanzo Gary L. Gray, *Engineering Mechanics: Statics and Dynamics*, Second. McGraw Hill, 2012, ISBN: 978-0-07-757061-3.
 - [19] R. Lamb. “How reel mowers work.” (2008), [Online]. Available: <https://home.howstuffworks.com/reel-mower.htm>.
 - [20] “Pedal power.” (2011), [Online]. Available: <https://www.sciencelearn.org.nz/resources/1348-pedal-power>.
 - [21] “Aluminum 6061-t6; 6061-t651.” (), [Online]. Available: <https://asm.matweb.com/search/SpecificMaterial.asp?bassnum=ma6061t6>.
 - [22] “Factors of safety - fos - are important in engineering designs.” (2010), [Online]. Available: https://www.engineeringtoolbox.com/factors-safety-fos-d_1624.html.
 - [23] A. M. S. Richard G. Budynas, *Rourke's Formulas for Stress and Strain*, Ninth. McGraw Hill, 2020, ISBN: 978-1-26-045376-8.
 - [24] “Aluminum tubing 1/8” through 12-3/4” od tube.” (), [Online]. Available: <https://www.vitaneedle.com/aluminum-tube>.
 - [25] M. Jhung and J. Jo, “Equivalent material properties of perforated plate with triangular or square penetration pattern for dynamic analysis,” *Nuclear Engineering and Technology*, vol. 38, Jan. 2006.
 - [26] A. D. Alba. “The dangers of hot sand.” (2019), [Online]. Available: <https://www.13newsnow.com/article/news/local/the-dangers-of-hot-sand/291-22994ef3-f3f6-440a-9949-d2f9b549e455>.
 - [27] “Bicycle aluminum alloys 6061 and 7005.” (2018), [Online]. Available: <https://aluminium-guide.com/en/velosipednaya-rama-alyuminievye-splavy-6061-i-7005/>.
 - [28] M. P. M.Satheesh.1, “Flexural strength behavior of al 6061matrix reinforced with sic and coconut shell ash,” [Online]. Available: <https://www.internationaljournalssrg.org/uploads/specialissuepdf/ICITSET/2018/ME/IJME-ICITSET-P103.pdf>.
 - [29] “Veva wheels.” (), [Online]. Available: <https://www.amazon.com/VEVOR-Beach-Balloon-Wheels-Replacement/>.
 - [30] “Commercial brush fillings — precision brush.” (), [Online]. Available: <https://precisionbrush.com/brush-fillings>.
 - [31] “Aluminum 6061-t6; 6061-t651.” (), [Online]. Available: <https://asm.matweb.com/search/SpecificMaterial.asp?bassnum=ma6061t6>.

-
- [32] “Steels, general properties.” (), [Online]. Available: <https://www.matweb.com/search/datasheet.aspx?bassnum=MS0001&ckck=1>.